NOVEL HISTONE DEMETHYLASE INHIBITORS SYNERGISTICALLY ENHANCE THE EFFECTS OF A DNA HYPOMETHYLATING AGENT IN BREAST CANCER CELLS

By

Benjamin R. Leadem

A dissertation submitted to The Johns Hopkins University in conformity with the requirements for the degree of Doctor of Philosophy

Baltimore, MD

March, 2015

I. Abstract

DNA methylation and histone methylation function together in the epigenetic regulation of gene expression, but these processes can be altered in cancer. Recently, the H3K4 demethylase, *KDM5B*, was shown to be amplified and overexpressed in luminal breast cancer, making it an ideal target for chemotherapeutic intervention. In this study, we characterized the phenotypic and molecular effects of a novel group of KDM5 inhibitors, either alone or in combination with the DNA demethylating agent 5-Aza-2'-deoxycytidine (DAC), in luminal breast cancer cells. We found that KDM5 inhibitors and DAC synergistically inhibit cell proliferation and induce apoptosis relative to each drug alone. Additionally, microarray analysis indicated that combination treatment with KDM5 inhibitors and DAC resulted in the significant upregulation of hundreds of genes relative to DAC alone. Among these targets was an enrichment for genes in immunomodulatory pathways which are upregulated after exposure to the DNA demethylating agent 5-azacytidine. We then analyzed whole genome DNA methylation levels using the Infinium 450k microarray and, when compared to DAC treatment alone, found no additional loss of DNA methylation in the combination treatment. Instead, upregulaton of target genes appears to be mediated, at least in part, by a specific increase in H3K4 trimethylation levels at the at target promoters following exposure to the KDM5 inhibitors. Our results indicate that target genes are regulated by both DNA methylation and histone methylation in breast cancer cells. Upregulation of these genes via combined KDM5 inhibitor and DAC treatment leads to the synergistic inhibition of proliferation and may represent an exciting new application for epigenetic therapy in the treatment of breast cancer.

Advisor: Stephen Baylin, M.D.

Reader: Robert Casero Jr., Ph.D.

II. Preface

Baltimore, March 2015

III. Table of Contents

IV. List of Tables

V. List of Figures

1. CHAPTER 1: INTRODUCTION

1.1 The epigenome of the normal cell

Epigenetics is defined as "the study of heritable changes in gene expression that occur independent of changes in the primary DNA sequence" (Holiday 1987). Furthermore, these changes are stable through several generations of cell replication. Upon being established during cellular differentiation, epigenetic changes mediate unique gene expression patterns, which in turn enable the development of distinct cell types despite each cell containing identical genetic information. Epigenetic modifications are manifested via changes in the chromatin structure, which is the way in which the genome is organized within the cell. The basic unit of chromatin is the nucleosome, which consists of 146 base pairs (bp) of DNA wrapped around an octamer of four paired histone proteins (H2A, H2B, H3, and H4). These units are repeated throughout the genome, and assume a compact, higher order structure. This organization plays a critical role in the regulation of gene expression, as a looser, more open chromatin structure allows for transcription factor binding and gene expression. Conversely, a tight chromatin structure prevents binding of transcriptional activators and results in gene repression (Mikkelsen et al. 2007, Guenther & Young 2010). The epigenetic mechanisms that mediate these alterations to the chromatin architecture can be divided into four general classes: methylation of cytosine bases in DNA, post-translational modifications to histone proteins, nucleosome remodeling, and non-coding RNA's. Here, we will focus on the effects of DNA methylation and histone modification.

The most intensely studied of these four types of epigenetic modifications is DNA methylation; it is the mechanism responsible for the stable silencing of genes, thereby

allowing the maintenance of cellular identity. In mammals, although methylation of either cytosine or adenine have been observed, methylation of cytosines residing in CpG dinucleotides is far more common (Bird 2002). A high preponderance of these dinucleotides are found clustered either at the 5' end of a gene or within repetitive regions of the genome. Furthermore, when adjacent to genes, CpGs are often found within regions called CpG islands, which are defined as areas greater than 200 bases long with GC content greater than 50% and a high relative density of CpG (>0.6 over expected). CpG islands are found within 60% of all gene promoters, and although the vast majority remains in an unmethylated state in normal cells, methylation of these regions leads to stable gene silencing (Jaenisch et al. 1985, De Smet et al. 1996, Bird 2002). Regardless of location, this silencing is mediated by the recruitment of co-repressor proteins, such as histone deacetylases (HDAC's), via protein complexes containing methyl-binding proteins such as MBD's or MeCP2 (Jones et al. 1998). These proteins mediate a closed chromatin structure, which in turn, prevents recruitment of transcriptional activators, such as c-myc (Pendergrast et al. 1988).

DNA methylation patterns are established during development and are mediated by a set of proteins called DNA methyltransferases (DNMTs). In mammals, there are four known DNMT proteins: DNMT1, DNMT3A, DNMT3B, and DNMT3L. Canonically, DNMT3A and DNMT3B are considered the *de-novo* methyltransferases; these two proteins are responsible for catalyzing the establishment of new DNA methylation patterns within the genome. The mechanism for this process is unknown and is currently the subject of intense investigation. DNMT1, on the other hand, has been described as the maintenance methyltransferase, as during cellular replication, DNMT1 is

recruited to the newly synthesized, hemi-methylated DNA and catalyzes the completion of methylation of the newly synthesized strand. Furthermore, DNMT1 has recently been shown to mediate gene repression independent of its catalytic activity via the recruitment of co-repressor proteins such as KDM1A (LSD1) (Clements et al. 2012).

Until recently, DNA methylation was considered to be an irreversible modification to the DNA, but the characterization of a family of proteins known as the ten-eleven translocation (TET) proteins, has suggested that DNA methylation is more plastic than once thought (Figueroa et al. 2010). These proteins catalyze the conversion of methylated cytosine to hydroxymethylated cytosine via an alpha-ketoglutarate dependent step, which through several subsequent enzymatic reactions, results in the restoration of an unmodified cytosine (Williams et al. 2011). These are the first enzymes known to actively demethylate DNA and are critical in the maintenance of DNA methylation equilibrium. Indeed, a recent study found that neomorphic mutations to isocitrate dehydrogenases (IDH) result in a substantial increase of 2-hydroxyglutarate, a co-factor that inhibits TET activity and could lead to a subsequent buildup of DNA methylation (Figueroa et al. 2010). Although these proteins are currently the subject of intense investigation, it is clear that the TET proteins play an essential role in the establishment and maintenance of DNA methylation patterns.

The other epigenetic mechanisms discussed here are the post-translational modifications of histone proteins. The C-terminus region of histones is hydrophobic and is folded into the core of the nucleosome, but the N-terminal region is hydrophilic, and accessible for protein binding. These N-terminal "tails" are substrates for covalent modifications including: acetylation, methylation, phosphorylation, ubiquitination, and

sumoylation, though methylation and acetylation are by far the best understood of these modifications. Canonically, acetylation of lysine residues in these histone tails by histone acetyltransferases (HATs) is associated with transcriptional activation (Kouzarides 2007). Conversely, methylation of histone tail lysines is more complex and can either lead to gene repression or activation depending on which specific residue in the tail is modified. For example, methylation of histone 3 lysine 9 (H3K9) or lysine 27 (H3K27) localize to the promoters of transcriptionally repressed loci, whereas histone 3 lysine 4 (H3K4) methylation is often found at the promoters of genes undergoing active transcription (Kouzarides 2007). The repressive functions of H3K9 or H3K27 methylation are mediated by the recruitment of co-repressor complexes, such as HP1 or Polycomb repressive complex 1 (PRC1), leading to the establishment of a compact, heterochromatic state (Aagard et al. 1999, Fischle et al. 2003). Conversely, active methylation marks, such as H3K4, mediate transcriptional activation via recruitment of transcriptional activating complexes such as the HAT complex SAGA (Timmers et al. 2005).

Although histone methylation was once thought to be an irreversible epigenetic modification, it is now apparent that a dynamic equilibrium for each mark is maintained by a unique set of "writer" histone methyltransfersase (HMTs) and "eraser" lysine demethylases (KDMs). The repressive methylation of H3K27 is catalyzed by the Polycomb Repressive Complex Group 2 (PRC2) member EZH2 (Czermin et al. 2002), whereas H3K9 methylation is catalyzed by the cooperative action of G9a and G9a related protein (GLP) (Tachibana et al. 2005). Conversely, the JMJD family of lysine demethylases have been shown to actively demethylate H3K9 tails, and KDM6a and

KDM6b catalyze the removal of H3K27 methylation (Sengoku et al. 2011, Couture et al. 2007)

Similarly, equilibrium of the active H3K4 methylation marks is maintained by a balancing set of HMT and KDM proteins. H3K4 methylation is catalyzed by the mixed lineage leukemia (MLL) like family of proteins which includes: SET1A, SET1B, MLL1, MLL2, MLL3, and MLL4 (Ruthenburg et al. 2007). These enzymes catalyze the mono, di, and trimethylation of H3K4. Removal of H3K4 methylation is catalyzed by two distinct classes of enzymes, each with a unique mechanism of action. First, KDM1A (LSD1) actively removes mono and dimethylated, but not trimethylated, H3K4 via an FAD dependent amine oxidation step (Shi et al. 2004). Recently, the Jumonji domain containing KDM5 proteins have been shown to be capable of removing all three methylation states via an alpha-ketoglutarate dependent oxidation reaction (Yamane et al 2007, Klose et al. 2007). The KDM5 proteins will be discussed in greater detail in the next chapter.

Much like DNA methylation, the distribution of these histone modifications changes during the differentiation process of a cell. In embryonic cells, a "bivalent" state has been characterized at a number of genes in which both active and repressive histone methylation marks are simultaneously found surrounding transcription start site regions (Bernstein et al. 2006, Mikkelsen et al. 2007). This balance is thought to maintain a weakly repressed, but poised transcriptional state, thereby allowing close regulation of gene expression during various developmental processes. Upon differentiation, the bivalent state of these genes is lost, as most promoters in differentiated cells contain exclusively active, or repressive histone modifications.

These epigenetic mechanisms are not mutually exclusive of each other, in fact DNA methylation and histone modification are functionally interconnected and act in concert to exert combinatorial effects on chromatin structure and gene expression. First, aside from its main catalytic function, DNTM1 has been shown to serve as a scaffolding protein for the recruitment of other co-repressor proteins such as HDACs and KDM1a (Clements et al. 2012). Conversely, HMTs, such as the H3K9 HMT G9a, have been shown to directly interact with DNMTs and recruit them to binding sites (Tachibana et al. 2009) to facilitate further gene silencing. Furthermore, the epigenetic modifications themselves can modulate DNMT localization; in ES cells, prior to establishment of DNA methylation patterns, methylation of H3K4 blocks recruitment of the catalytically inactive DNMT3L, which in turn prevents recruitment of the *de novo* methyltransferases DNMT3A and DNMT3B (Ooi et al. 2007). Additionally, a close association between H3K27 methylation patterns and DNA methylation have been described, as promoter regions marked by H3K27 methylation, and/or bivalent chromatin in ES cells are commonly aberrantly DNA hypermethylated in cancer (Ohm et al. 2007, Schlesinger et al. 2007). Finally, several studies have functionally demonstrated the interconnectivity of these epigenetic mechanisms, as upon administration of an inhibitor of DNA methylation, histone methylation patterns throughout the epigenome are dramatically reorganized (Lambrot & Kimmins 2010, Komashko & Farnham 2010). Specifically, the repressive histone modifications H3K9me3 and H3K27me3 are lost from target promoters following AZA treatment (Komashko & Farnham, 2010). These findings indicate that the epigenetic regulation of transcriptional activity is subject to several layers of regulation, and perturbations in one pathway can have significant effects on the other.

1.2 Epigenetic changes in cancer

It is now well understood that cancer, alone with genetic perturbations, can be characterized by gross alterations within the epigenome. These changes manifest in the nucleus with unique chromatin structure, which in turn leads to global differences in gene expression patterns compared to the normal cell. Currently, the best understood altered epigenetic mechanism is DNA methylation. First observed in the 1980's, cancer is characterized by global intergenic DNA hypomethylation with focal DNA hypermethylation of CpG islands within gene promoters (Jones & Baylin, 2002). Like genetic mutations, these changes to the epigenome, or epimutations, can lead to the activation of proto-oncogenes or the silencing of critical tumor suppressors. Global hypomethylation of repetitive regions in the genome allows a more open and accessible chromatin structure, and given the repetitive nature of the DNA sequence, this accessibility can lead to genomic instability and chromosome rearrangement (Eden et al. 2003). Furthermore, hypomethylation can lead to the aberrant activation of proto-oncogenes such as R-Ras or S-100 (Wilson et al. 2007). Conversely, focal gains of DNA methylation promoter CpG islands can lead to the stable silencing of critical tumor suppressor genes. This phenomenon was first observed with the aberrant silencing of the tumor suppressor *Rb* in retinoblastoma, and has now been observed in a number of other cancer types other well at well known tumor suppressor genes such as: *BRCA1*, *CALC1*, *MLH1*, *p16*, and *VHL* (Greger et al. 1989, Nelkin et al. 1991, Baylin 2005). Interestingly, a recent study found that whereas these focal gains in promoter CpG island methylation are maintained during intra-tumor development from primary tumor to metastasis, the previously described globally hypomethylated regions are not consistently maintained

during this clonal expansion (Aryee et al. 2012). These findings indicate that, much like genetic mutations, promoter methylation can be a critical "driver" event in human carcinogenesis.

The mechanism behind these aberrant DNA methylation profiles remains unclear. One potential explanation for this phenomenon could be that the *de-novo* methyltransferases are targeted to specific regions via alterations to the histone code, as aberrantly hypermethylated genes in cancer are commonly unmethylated and marked with H3K27 methylation in ES cells (Ohm et al. 2007, Schlesinger et al. 2007). Another intriguing hypothesis stems from an alteration to DNA methylation equilibrium. As described above, mutations to *IDH1* and *IDH2* are often found in gliomas, and subsequently lead to the inactivation of TET proteins. This inactivation prevents the active removal of cytosine methylation; accordingly, *IDH1* mutations are associated with a CpG island hypermethylator phenotype (CIMP) (Figueroa et al. 2010).

Similarly, global alterations in histone modifications have been associated with cancer as well. Global hypoacteylation of H4 in a number of cancer types is mediated by the overexpression of HDACs, leading to the aberrant repression of transcriptional activity (Halkidou et al. 2004, Song et al. 2005). Furthermore, histone methylation patterns throughout the genome are often altered during tumorigenesis. Aberrant increases in H3K9 or H3K27 methylation result in the repression of key genes; similarly cancer specific decreases in promoter H3K4 methylation have also been found at these repressed loci (Nguyen et al. 2002, Valk-Lingbeek et al. 2004, Cloos et al. 2008). These changes are mediated by perturbations to either the HMTs responsible for placing these marks, or the KDMs responsible for removing them. For example, overexpression of the

H2K27 methyltransferase EZH2 has been observed in a number of cancers (Valk-Lingbeck et al. 2004). Similarly, overexpression of the H3K4 demethylases KDM1A and the KDM5 family of proteins have also been described in several cancer types (Yamane et al. 2007, Xiang et al. 2007). The role of the KDM5 proteins in tumorigenesis will be discussed in greater detail in the next chapter.

1.3 Epigenetic therapies in the treatment of cancer

Although epigenetic modifications are stable through several generations of cell division, the global alterations in epigenome during differentiation or tumorigenesis demonstrate that these marks are fundamentally reversible. As discussed in the previous section, epimutations can be key drivers in the development of cancer via the aberrant silencing of tumor suppressor genes. Thus these epimutations are ideal candidates for therapeutic intervention. Furthermore, given that any given cancer harbors hundreds of epimutations, which in turn results in the dysregulation of dozens of cell signaling pathways, targeting dysfunctional cancer epigenetic mechanisms for therapeutic intervention could hypothetically correct these aberrant processes, thereby leading to a potent and durable anti-cancer response. But, unlike other chemotherapeutic regiments, the goal of epigenetic therapy is not purely cell death via cytotoxicity induced by high drug doses. Instead, the ultimate goal here is the restoration of normal cell gene expression and signaling patterns, thereby reprogramming the cancer cell to a more normal state. Until very recently, epigenetic therapies could be divided into two distinct categories: DNA demethylating agents and HDAC inhibitors. Both are discussed below.

Additionally, new drugs have been developed recently that target the various HMTs and KDMs; these too are discussed below.

Originally developed as cytotoxic chemotherapy agents in the 1960s, cytidine analogs, such as 5-azacytidine (AZA) and 5-aza-2'-deoxycytidine (DAC), were later found to possess DNA demethylating activity (Jones & Taylor. 1980). Given that these compounds are nucleoside analogs, they are readily incorporated into the genome, and upon recruitment of the DNMTs to these sites of integration, AZA and DAC covalently bind and irreversibly inhibit the catalytic activity each of the three active DNMTs (Jones & Taylor, 1980). This binding then triggers the degradation of the protein, resulting in the net loss of methylation throughout the genome over several rounds of cell division. Specifically, promoter demethylation and the subsequent re-expression of a number of tumor suppressor genes, such as p16 and APC, have been observed in a number of cancer types following treatment with either AZA or DAC (Astsaturov et al. 2010). Initially though, the promise of these compounds seemed limited. Like other cytotoxic agents, the first clinical trials of these compounds utilized relatively high doses, which resulted in significant toxicity, likely due to substantial DNA demethylation and other unknown off-target effects (Issa et al. 2005). But, it was later discovered that the lower doses of these compounds, which do not induce significant toxicity, retain their intrinsic DNMT inhibitory activity and can be efficacious in the treatment of hematologic malignancies (Tsai et al. 2011). Currently, AZA is FDA approved for the treatment of myelodysplasia, and DAC is approved for the treatment of myelodysplasia and acute myelogenous leukemia (AML). Although clinical efficacy of these compounds in the treatment of

solid tumors is not as readily apparent as in the treatment of hematologic malignancies, this is currently an area of intense investigation.

The other major class of existing epigenetic drugs is the HDAC inhibitors. As described above, HDACs are commonly overexpressed in a number of cancers, resulting in the hypoacetylation of the chromatin, resulting in a tight conformation that represses transcriptional activity. Four different types of HDAC inhibitors have been developed: short chain fatty acids (Valproic acid), hydroxamic acids (Vorinostat), cyclic tetrapeptides (Romidepsin), and benzamides (Entinostat), each with unique functional groups, but all inhibit the catalytic activity of HDACs, thereby resulting in the accumulation of acetylated histones. Although the exact antitumor mechanism of action of these inhibitors is unclear, HDAC inhibitor treatment has been shown to induce expression of the cell cycle regulator p21, as well as activating intrinsic and extrinsic apoptotic signaling pathways (Rocchi et al. 2005, Peart et al. 2005). Nevertheless, these agents have been proven to be clinically effective in the treatment of hematological malignancies, as Romidepsin has been approved for the treatment of peripheral and cutaneous T-cell lymphomas, and Vorinostat has also been approved for the treatment of cutaneous T-cell lymphoma (Piekarz et al. 2009). Despite these successes, several challenges remain which prevent the use of these compounds in the treatment of more common cancer types. First, much like the nucleoside analogs, high doses of these compounds induce significant cytotoxity, likely caused by the extensive DNA damage resulting from treatment with these compounds (Robert et al. 2012). Furthermore, other off target effects of these compounds are possible, as HDACs have been shown to remove acetylation from other proteins besides histones, such as the tumor suppressor

protein p53 (Solomon et al. 2006). Given these challenges, the potential clinical efficacy of combining these compounds with other chemotherapeutic agents, including DNA demethylating agents, is currently being explored.

Given the lack of clinical success of these epigenetic therapeutic agents in the treatment of solid tumors, one exciting avenue of exploration is the potential efficacy that could be achieved by combining these agents with either other epigenetic inhibitors or existing chemotherapeutic agents. *In-vitro* work has shown that combining DAC and the HDAC inhibitor Trichostatin A (TSA) synergistically reactivates a number of stably silenced genes (Cameron et al. 1999). This paradigm of treatment has recently shown promise of efficacy in a phase 1/2 trial for the treatment of non-small cell lung cancer (NSCLC) (Jeurgens et al. 2011). Furthermore, recent studies have suggested that combining epigenetic therapy with existing chemotherapeutic agents might induce a significantly better clinical response. First, AZA and DAC have been observed to restore sensitivity to carboplatin in ovarian cancers previously resistant to platinum based chemotherapeutic agents (Fu et al. 2011). Second, combining the HDAC inhibitor vorinostat with carboplatin and paclitaxel resulted in a significantly increased response rate in the treatment of NSCLC (Ramalingam et al, 2010). Third, when combined with an aromatase inhibitor, Exemestane, in the treatment of breast cancer, the addition of entinostat resulted in significant increases in overall survival (Yardley et al. 2011). Finally, although still in the preclinical phase, an exciting new area of investigation has been the potential clinical efficacy of combining AZA with immune checkpoint therapy targeting PD-L1/PD-1. Recent studies have shown that AZA re-sensitized NSCLC cells

to immunotherapy, potentially indicating an efficacious new treatment paradigm (Wrangle et al. 2013).

Recent years have witnessed an explosion of interest in the development of chemical inhibitors of other epigenetic mechanisms. As described above, histone methylation patterns are grossly perturbed in a number of cancer types as a result altered activity of either HMTs, such as EZH2, or KDMs, such as the KDM5 family of proteins. Recently, potent inhibitors of an EZH2 variant containing a gain of function mutation have been developed for the treatment of leukemias and are nearly in clinical trials (McCabe et al. 2012). Similarly, given that accumulation of H3K9 methylation has been associated with increased DNMT recruitment, development for inhibitors of the H3K9 methyltransferases G9a & GLP are currently underway (Fahrner et al. 2002). Finally, overexpression of two classes of H3K4 demethylases, KDM1A and the KDM5 family, has been observed in several cancer types (Kahl et al. 2006, Yamane et al. 2007, Hayami et al. 2011). Furthermore, both classes of demethylases have been shown to possess oncogenic functions in a number of cancer types (Yamane et al. 2007, Hayami et al. 2011, Lin et al. 2011). Accordingly, inhibitors of KDM1A have been developed and both preclinical and clinical investigations are underway. Here, we characterize a novel set of inhibitors of the KDM5 family of proteins.

1.4 Research outline

As described above and in the subsequent chapters, the KDM5 family of H3K4 demethylases are overexpressed in a number of cancers. Specifically, *KDM5B* was shown to be genetically amplified and overexpressed in luminal breast cancer, making it

an ideal target for therapeutic intervention (Yamamoto et al. 2014). In this study, we characterized the phenotypic and molecular effects of a novel group of KDM5 inhibitors, either alone or in combination with the DNA demethylating agent 5-Aza-2'-deoxycytidine (DAC), in luminal breast cancer cells. We have designated three major aims in this study; first, we characterize the effects of the KDM5 inhibitors on the epigenome by measuring global levels of various histone marks and histone modifying enzymes. Furthermore, we determined the effects these changes exert on cell proliferation. Second, we assess the potential for the KDM5 inhibitors to enhance the phenotypic effects of DAC. Specifically, can KDM5 inhibition synergize with DAC to inhibit proliferation of luminal breast cancer cells? Finally, we characterize the molecular effects associated with treatment with the KDM5 inhibitors alone and in combination with DAC.

2. CHAPTER 2. *IN-VITRO* CHARACTERIZATION OF KDM5 INHIBITORS IN LUMINAL BREAST CANCER CELLS

2.1 Introduction

As described in the previous chapter, the KDM5 family of histone demethylases catalyzes the removal of H3K4me3 and H3K4me2, both of which are associated with transcriptional activation. The family is comprised of 4 homologs: KDM5A (also known as RBP2 or JARID1A), KDM5B (also known as JARID1B or PLU-1), KDM5C (also known as JARID1C OR SMCX), and KDM5D (also known as JARID1D or SMCY), of which, KDM5A and KDM5B have been studied in much greater depth than the remaining family members. Both KDM5A and KDM5B have been described as critical regulators of tumorigenesis. Previous studies have shown that KDM5A promotes cancer cell growth, inhibits cellular senescence & differentiation (Klose et al. 2007), silences the expression of critical cell cycle regulators (Benevolenskaya et al. 2005), and is overexpressed in gastric cancer (Zeng et al. 2010). Similarly, KDM5B is overexpressed in cancers of the breast, skin, lung, bladder, and prostate (Xiang et al. 2007, Yamamoto et al. 2014). Loss of KDM5B leads to suppression of growth in a number of cancer cell lines (Hayami et al. 2010, Yamamoto et al. 2014). Furthermore, loss of either KDM5A or KDM5B leads to decreased tumorigenesis in xenograft and transgenic mouse models of cancer (Yamane et al, 2007, Lin et al. 2011). Due to these potentially oncogenic functions, KDM5A and KDM5B are ideal candidates for targeted chemical inhibition via small molecules.

With the above potential implications for tumorigenesis in mind, Constellation Pharmaceuticals developed a series of small molecules designed to inhibit the catalytic

activity of the KDM5 family of proteins. We were kindly supplied with two "active" compounds, CPI-455 and CPI-766, with high measured affinity for the target KDM5 proteins, and as a control, one "inactive" compound with a similar chemical structure, CPI-203, which has a much lower affinity for KDM5 proteins. Here, we begin to test, in a panel of luminal breast cancer cell lines certain key cellular effects that could be relevant to the eventual therapeutic potential of these inhibitors. We chose this model as these cell lines have shown consistent sensitivity to loss of KDM5B function via genetic manipulation (Scibetta et al. 2008, Yamamoto et al. 2014). First, we characterized the histone modifying effects treatment with these compounds has on breast cancer cells by measuring global level of specific histone methylation marks. Next, we assessed the ability of these compounds to inhibit growth by measuring net cell proliferation following continuous exposure to each of the compounds in three luminal breast cancer cell lines: MCF-7, T-47D, and EFM-19.

2.2 Results

2.2.1 Exposure to active KDM5 inhibitors specifically increases H3K4 trimethylation

To determine the effects that KDM5 inhibitors have on H3K4 methylation, we incubated MCF-7 cells with increasing concentrations of each compound for 24 and 48 hours. Within 24 hours, increases in H3K4me3, but not H3K4me2, were observed after exposure to either of the two active compounds, CPI-455 and CPI-766, in a dose-dependent manner. Further increases in H3K4me3 levels were observed with 48 hours of treatment. Exposure to the inactive compound, CPI-203, resulted in no changes to either H3K4me3 or H3K4me2 levels (Fig. 2-1).

Next, we assessed the specificity of the KDM5 inhibitors for H3K4me3 by measuring global levels of several other H3 methylation marks via immunoblot. MCF-7 cells were exposed to 3 doses of CPI-766 for 24 and 48 hours. No changes were observed in H3K27me2, H3K27me3, H3K9me2, or H3K36me2 at either time point (Fig. 2-2).

2.2.2 Exposure to KDM5 inhibitors results in post-translational stabilization of KDM5b

Given that LSD1 (KDM1A) is capable of demethyating H3K4me2, and potentially functionally compensating for loss of function of the KDM5 proteins, global protein levels of LSD1 were assessed after exposure to CPI-766 for 24 and 48 hours. Global levels of KDM5A and KDM5B were also measured. No changes in LSD1 or KDM5A were detected, but dramatic increases in KDM5B protein levels were observed

(Fig. 2-3a). This increase was also seen after exposure to CPI-455, but not after exposure to the inactive compound, CPI-203 (Fig. 2-3b). To determine if exposure to the active KDM5 inhibitors upregulated transcription of KDM5B, mRNA levels were measured by quantitative RT-PCR after 72 hours of exposure to each of the KDM5 inhibitors. Slight increases in transcript levels were detected after exposure to the active inhibitors (Fig. 2-3c). These data suggest that the increase in KDM5B levels are likely not a result of transcriptional upregulation, but rather post-translational stabilization of the protein.

2.2.3 IC_{50} Calculation for KDM5 inhibitors in luminal breast cancer cell lines

To assess the effects that the KDM5 inhibitors have on cell proliferation, dose response curves were generated for all three compounds in three luminal breast cancer cell lines. In all cell lines tested, CPI-455 and CPI-766 exhibited similar dose dependent effects on cell proliferation. In MCF-7 and T-47D, the inactive compound, CPI-203, demonstrated very little effect on cell proliferation, whereas in EFM-19, decreased viability was observed at doses higher than 30uM (Fig. 2-4). IC_{50} values for each compound/cell line can be found in Table 2-1.

2.3 Discussion

Here, we set out to characterize the specificity and potency of KDM5 inhibitor compounds by measuring global levels of H3K4 methylation marks, as well as other histone methylation marks. We found that within 24 hours, global levels of H3K4me3, but not H3K4me2, drastically increase with as little as 1 uM of the active compounds. Although KDM5A and KDM5B have both been shown to catalyze the removal of all three H3K4 methyl states in previous studies, these results were found in overexpression models, and thus may not represent the most biologically relevant systems. Indeed, a recent study found that knockdown of KDM5B resulted in global increases in H3K4me3, but not H3K4me2 (Yamamoto et al. 2014). These data suggest that H3K4me2 equilibrium is likely maintained through functional compensation by another histone demethylase, potentially KDM1 (also known as LSD1). Furthermore, the above data indicate that the KDM5 proteins are an essential regulator of H3K4me3, and the active compounds are potent inhibitors of these proteins. Next, we assessed the specificity of this H3K4me3 effect by measuring global levels of other histone marks. Given that no changes in the tested marks were observed, catalytic activity of other histone demethylases do not appear to be affected by treatment with these compounds. Thus, these compounds appear to be specific for the KDM5 proteins.

Given that H3K4me2 levels were unaffected by treatment with the KDM5 inhibitors, we next tested if functional compensation for loss of KDM5 catalytic function was mediated by an increase in protein levels of LSD1. No changes in LSD1 levels were observed after inhibitor treatment, which suggests that if LSD1 is compensating for loss of KDM5 function, it is likely through increased catalytic activity. Interestingly, marked

increases in KDM5B levels were observed at all tested doses. Minimal changes in KDM5B mRNA levels were detected, indicating that KDM5 inhibitor treatment leads to stabilization of the protein via an unknown post-translational mechanism.

Next, we tested the effects of each of the KDM5 inhibitors has on breast cancer cell proliferation. Given that several previous studies observed growth inhibition following protein knockdown of KDM5B in cancer cell lines, we hypothesized that we would see a similar pattern upon exposure to the KDM5 inhibitors. Interestingly, when exposed to concentrations that mediate drastic global increases in H3K4me3 levels, no significant changes in proliferation were observed in any of the cell lines tested. The compounds used here inhibit the catalytic activity of the KDM5 proteins and increase the protein levels of KDM5B, thus suggesting that loss of the KDM5 protein and their potential scaffolding functions may be required to mediate the reduction in viability observed in previous studies. Furthermore, very high doses of the active compound, but not the inactive compound, lead to a precipitous decrease in cell viability. These data suggest that either a very high threshold for global H3K4me3 levels must be crossed before viability is effected, or that the KDM5 inhibitors have unknown off-target effects at high doses that mediate the observed decrease in proliferation. Regardless, given that decreases in viability were only observed at doses that would be impossible to achieve *in-vivo*, the luminal breast cancer cell lines tested here do not appear to be especially sensitive to the loss of KDM5 catalytic activity *in-vitro.*

2.4 Materials and methods

2.4.1 KDM5 Inhibitors

Two active KDM5 inhibitor compounds, CPI-455 and CPI-766, and one inactive control compound, CPI-203, were obtained from Constellation Pharmaceuticals. All compounds were dissolved in DMSO to a final concentration of 10 mM. Eluted drug was stored at -20°C.

2.4.2 Cell lines

MCF-7, T-47D, and EFM-19 are luminal breast cancer cells. MCF-7 was grown in MEM supplemented with 10% fetal bovine serum (FBS), T-47D and EFM-19 were grown in RPMI 1640 supplemented with 10% FBS. All cell lines were incubated at 37°C with a 5% CO_2 atmosphere.

2.4.3 Effects on histone marks and histone demethylases

MCF-7 cells were treated with continuous exposure to the indicated KDM5 inhibitor for either 24 or 48 hours in MEM media supplemented with 2% FBS. Doses used are indicated in the figures; each experiment contained a DMSO mock control containing an equal final percentage of DMSO as treated cells. Total percentage of DMSO (0.5%) was normalized across all treatment groups. Following treatment, cells were harvested, pelleted, and stored at -20°C.

2.4.4 Western blotting and antibodies

Cell pellets were lysed in 4% SDS and the lysate was homogenized using Qiashredder columns (Qiagen #79656). Protein content was quantified using bicinchoninic acid (BCA) protein assay (Thermo #23225). Western blotting was performed as previously described (Cai et al. 2014)

The following primary antibodies were used: anti-trimethyl H3K4 (Cell Signaling #9751S), anti-dimethyl H3K4 (Millipore #07-030), anti-trimethyl H3K27 (Millipore #07-449), anti-dimethyl H3K27 (Upstate #07-452), anti-dimethyl H3K9 (Millipore #07-212), anti-dimethyl H3K36 (Upstate #07-274), anti-H3 (Abcam #ab1791), anti-KDM5B (Bethyl #A301-813A), anti-KDM5A (Cell Signaling #3876S), anti-LSD1 (Upstate #05-939), and anti-beta actin (Sigma #A2547). The following secondary antibodies were used: anti-Mouse IgG-HRP (GE #NA931V) and anti-Rabbit IgG-HRP (GE #NA934V).

2.4.5 Analysis of gene expression

Total RNA was extracted using Qiagen RNeasy RNA extraction kit (#74104). cDNA was produced using Life Technologies Superscript III First Strand Synthesis kit (#1080051). Quantitavive-PCR (qPCR) reacctions contained Applied Biosystems POWER SYBR Green Real-Time PCR Master Mix (#4367659), specific primers, cDNA, and water. All reaction were run on ABI StepOnePlus real-time PCR system. Relative quantitation of each target was calcuclated via the ΔΔCT method. Primer sequences are listed in Appendix 1.

2.4.6 Cytotoxicity assay

Cells were plated in 96 well cell culture plates (MCF-7: $3x10^4$, T-47D: $5x10^4$, and EFM-19: $7.5x10^4$) in their normal media and allowed to rest 24 hours. Cells were treated in base media supplemented with 2% FBS at the doses indicated; in each experiment, each dose was repeated in three technical replicates. Total DMSO percentage (0.5%) was constant across all treatment groups. Cells were treated for a total of ten days; media was aspirated and replaced with fresh drug containing media on days 3 and 7. Following treatment, total cell viability was measured with Promega CellTiteer AQueous Non-Radioactive Cell Proliferation Assay (MTS) (#G5421). Data shown represent the mean across three independent replicates.

2.4.7 Statistical Analysis

IC_{50} was calculated in GraphPad Prism 6 software using a variable slope (four parameter) non-linear fit. Error bars shown represent the standard error of the mean (SEM) across three independent replicates.

2.5 Figures: Chapter 2

2.5.1 Figure 2-1. Treatment with active KDM5 inhibitors increases global H3K4 trimethylation, but not dimethylation

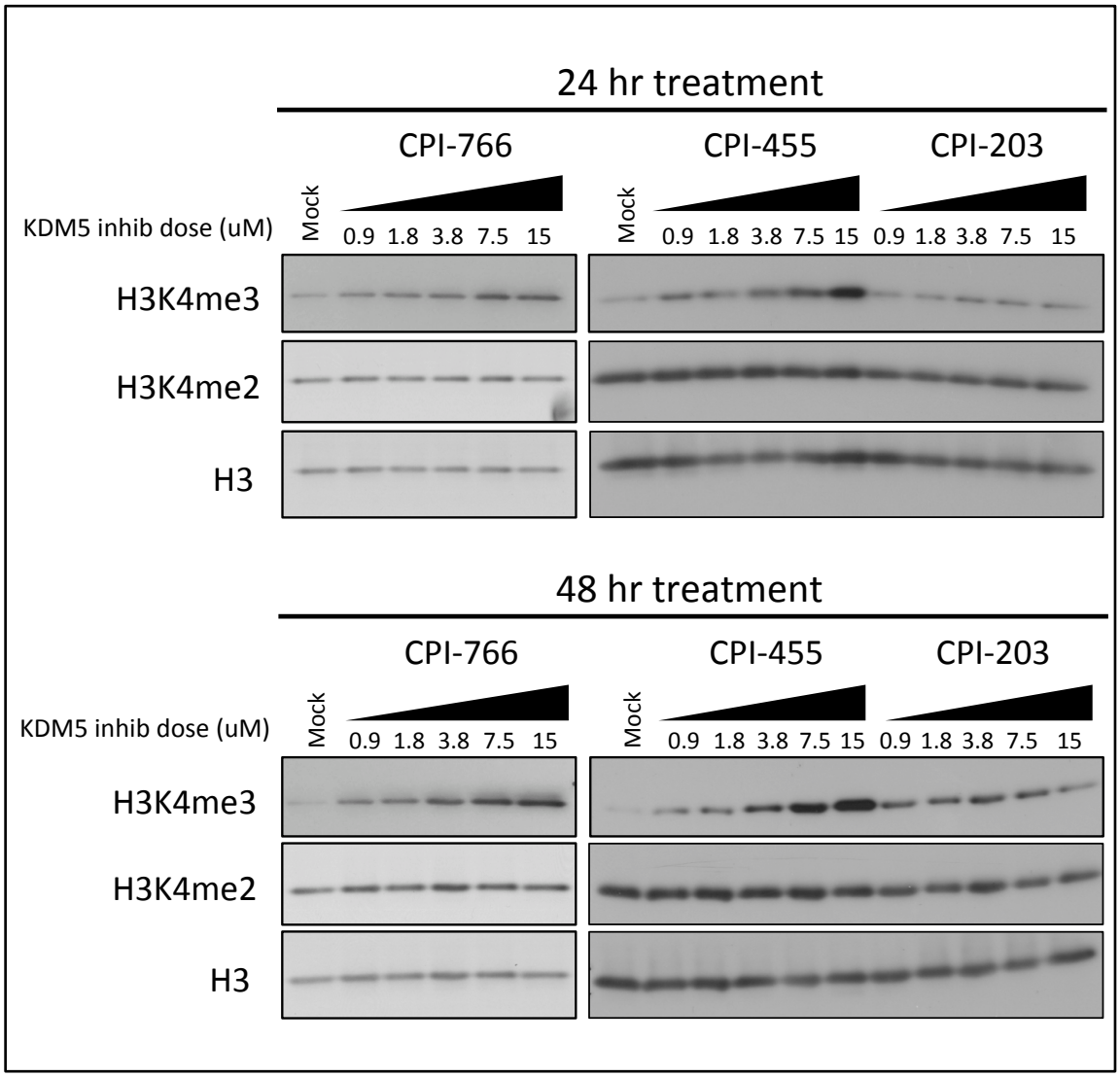

Figure 2-1. MCF-7 cells were exposed to the indicated drugs and doses for either 24 or 48 hours. Cells were immediately harvested and protein levels were assessed via immunoblot. H3 was used as a loading control.

2.5.2 Figure 2-2. Active KDM5 inhibitor has no effect on other tested histone marks.

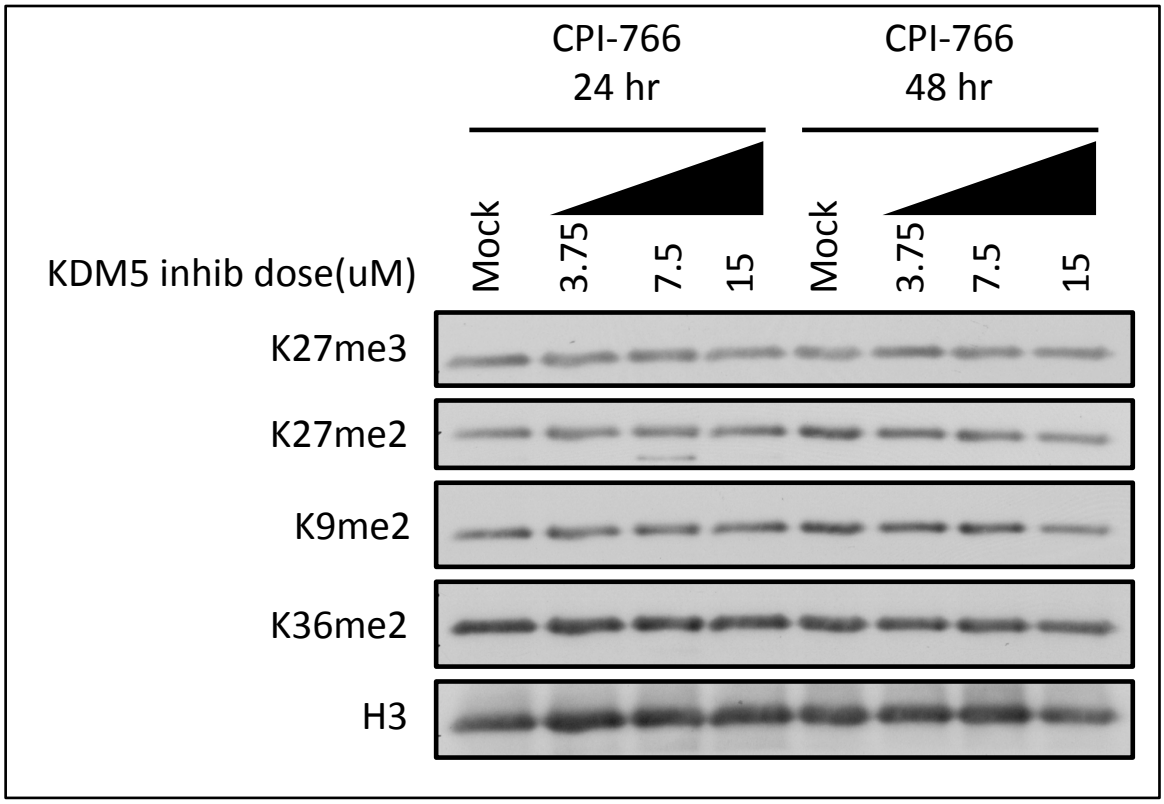

Figure 2-2. MCF-7 cells were exposed to CPI-766 for either 24 or 48 hours at the indicated doses. Cells were then immediately harvested and protein levels were assessed via immunoblot. H3 was used as a loading control.

2.5.3 Figure 2-3. Active KDM5 inhibitor treatment dramatically increases KDM5B protein levels

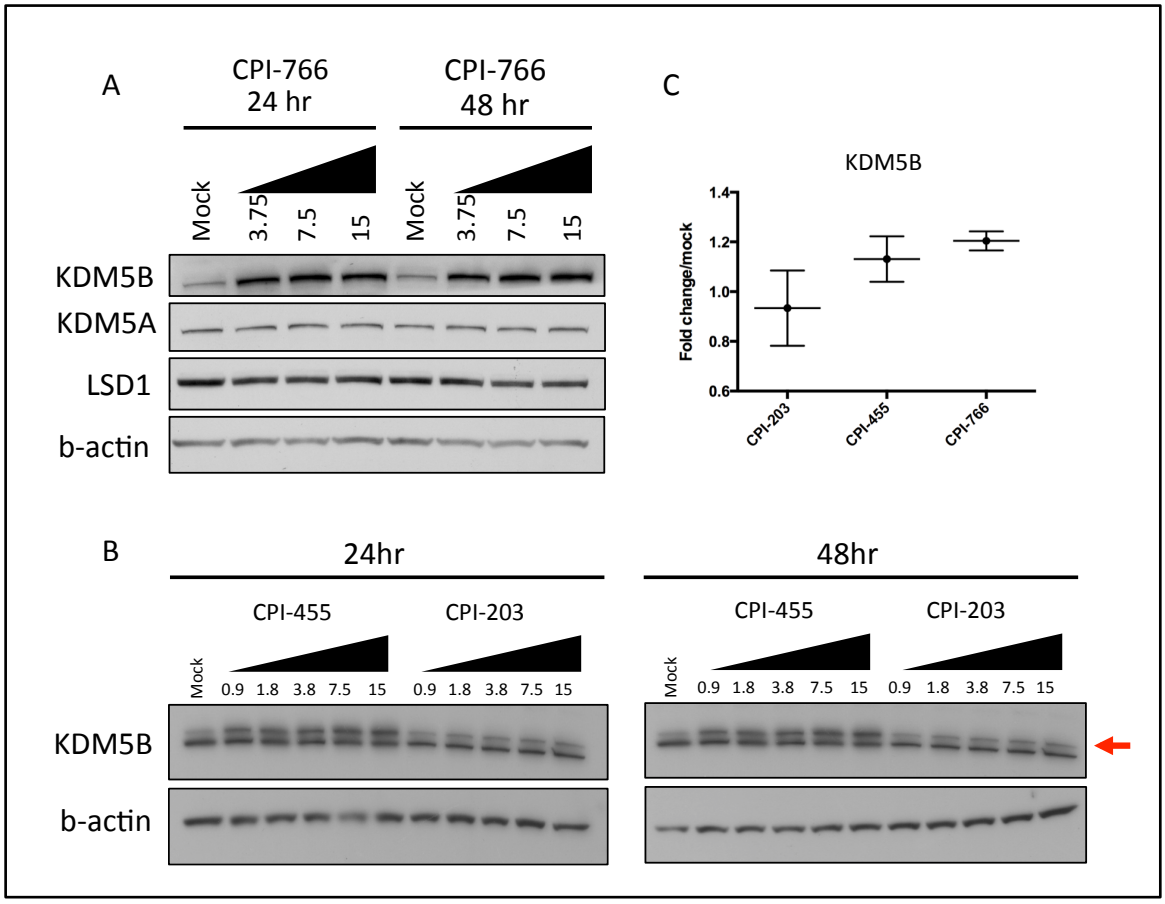

Figure 2-3. A&B. MCF-7 cells were exposed to the indicated compounds and doses for either 24 or 48 hours. Cells were then harvested and protein levels were assessed via immunoblot. Beta-actin was used as a loading control. C. MCF-7 cells were treated with 7.5 uM of indicated compound for 72 hours. KDM5B mRNA levels were measured via RT-PCR. GAPDH was used as a loading control locus. Error bars indicate standard deviation across technical replicates.

2.5.4 Figure 2-4. KDM5 inhibitor dose response curves in luminal breast cancer cell lines.

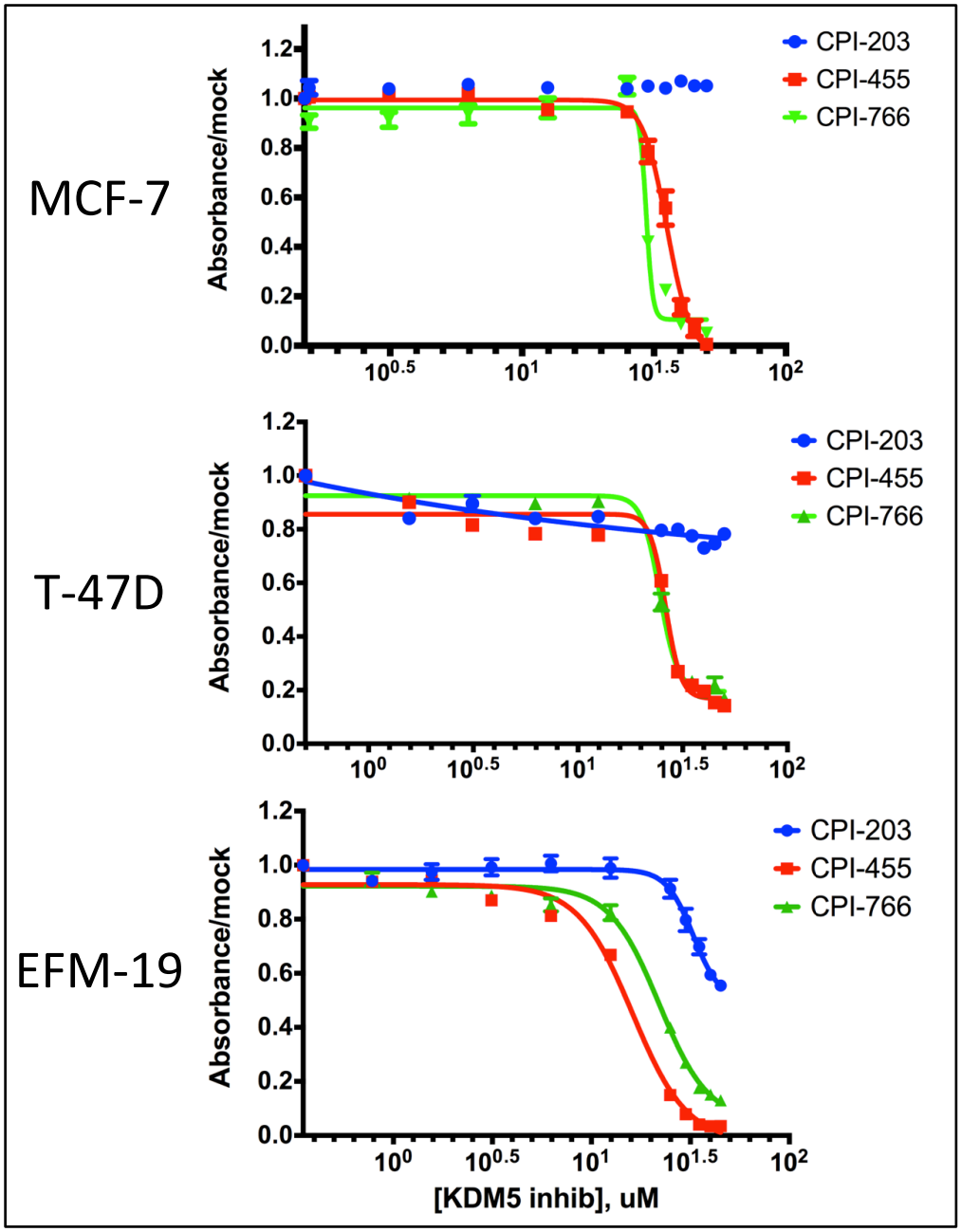

Figure 2-4. Cells were exposed to the indicated drug for 10 days. Viability was measured as percent absorbance relative to mock treated samples using MTS assay.

2.6 Tables: Chapter 2

2.6.1 Table 2-1. IC_{50} Calculation for KDM5 Inhibitors in 3 luminal breast cancer cell lines

	MCF-7	T-47D	EFM-19
CPI-203 (uM)	N/A	N/A	N/A
CPI-455 (uM)	35.40	26.19	16.13
CPI-766 (uM)	29.55	24.56	21.98

3. CHAPTER 3: *IN-VITRO* PHENOTYPIC EFFECTS OF COMBINATION TREATMENT WITH 5-AZA-2'-DEOXYCYTIDINE AND KDM5 INHIBITORS IN LUMINAL BREAST CANCER CELL LINES

3.1 Introduction

In Chapter 2, we introduced a novel set of KDM5 inhibitors that specifically increase global levels the active mark, H3K4me3, but do not affect breast cancer cell proliferation when administered alone. Given the potent effects of these compounds on H3K4 methylation, we were next interested in determining if chemical inhibition of KDM5 proteins could enhance, or even synergize, with the well-characterized DNA hypomethylating agent 5-aza-2'-deoxycytidine (DAC). Initial clinical applications utilizing relatively high doses of DAC and the related drug, 5-azacytidine (AZA), resulted in high toxicity in patients. However, more recently, low doses of these compounds have proven to be clinically efficacious in the treatment of hematological malignancies, and are now FDA approved for the treatment of myelodysplastic syndrome (Issa et al. 2005, Cashen et al. 2010). Clinical efficacy in the treatment of solid tumors has been far more elusive, and is currently the subject of intense investigation. DAC is a cytidine analog and upon incorporation into the genome, can inhibit all three active DNA methyltranserases (DNMT1, DNMT3a, DNMT3b) (Jones & Taylor, 1980). This action, especially at higher doses which are toxic if administered for more than 2 to days in-vitro, results in extensive global losses of DNA methylation (Jones & Taylor, 1980). Furthermore, *in-vitro* studies utilizing DAC or AZA, have demonstrated the interconnectivity between distinct epigenetic pathways, as upon administration of a DNA hypomethylating agent, histone methylation patterns throughout the epigenome are

dramatically reorganized (McGarvey et al. 2008, Lambrot & Kimmins, 2010, Komashko & Farnham 2010). Specifically, the repressive histone modifications H3K9me3 and H3K27me3 are lost from target promoters following AZA treatment (Komashko & Farnham, 2010). Additionally, methylation of H3K4 has been shown to block recruitment of DNMT3L, which in turn prevents *de novo* DNA methylation via the recruitment of DNMT3A and DNMT3B (Ooi et al. 2007). Given these findings, we hypothesize that the drastic increases in global levels of H3K4me3 mediated by KDM5 inhibition will further reorganize the chromatin architecture, thereby enhancing the effects of DAC.

Here, we assess the effects that combination treatment with DAC and the KDM5 inhibitor compounds has on cell proliferation in the same three luminal breast cancer cell lines utilized in the previous chapter. Specifically, we determined if these two classes of epigenetic therapeutic compounds can pharmacologically synergize to inhibit cell growth. Furthermore, we characterize the effects of combination treatment on induction of apoptosis and alteration of the cell cycle.

3.2 Results

3.2.1 KDM5 inhibitors synergize with DAC to inhibit proliferation

To determine if the KDM5 inhibitors could enhance the effects of DAC treatment, dose response curves were generated following combination treatment in the same three luminal breast cancer cell lines previously described in chapter 2. In all three cell lines, exposure to CPI-455 or CPI-766, but not CPI-203, following DAC resulted in a significant decrease in cell proliferation (MCF-7: $F=42.95$, $p<0.0001$; T-47D: $F=34.15$, $p<0.0001$; EFM=19: $F=52.55$, $p<0.0001$) (Fig. 3-1). Combination treatment IC_{50} values for each cell line are shown in Table 3-1.

Given these results, the potential for synergy between the KDM5 inhibitors and DAC was explored via calculation of combination index (CI) calculations. Furthermore, isobolograms were generated for each drug combination in all cell lines tested. DAC and CPI-455 demonstrated clear synergy at all effect levels in MCF-7 and EFM-19 as indicated by the CI values <1 and isobolograms shown in Figure 3-2 (Tab. 3-1)(Fig. 3-2a&c). In T-47D, DAC and CPI-455 demonstrated synergy at the highest effect levels, but were slightly antagonistic at the lower end of the dose range (Fig. 3-2b). With DAC and CPI-766 treatment, synergy or additivity were found at Fa levels <0.75 in all three cell lines (Fig 3-2). EFM-19 demonstrated clear synergy at all doses tested. All combination index values are listed in Table 3-1.

Furthermore, dose reduction index (DRI) values for DAC were calculated following combination treatment in order to assess the dose of DAC needed to achieve the same effect as when given alone. In MCF-7 combination treatment with either the KDM5 inhibitors resulted a slight reduction in the amount of DAC needed, as reflected

by DRI values for DAC in the range of 1.3-2.94. In T-47D and EFM-19, combination treatment resulted in robust reductions in the amount of DAC needed, with DRI values for DAC ranging from 1.88-19.43. All DRI values are show in Table 3-2.

3.2.2 Combination treatment significantly increases induction of apoptosis

To determine if the KDM5 inhibitors, either alone or in combination with DAC, could enhance apoptosis induction, two measures of apoptotic signaling were utilized; Poly (ADP-ribose) Polymerase (PARP) cleavage was measured via immunoblot and Annexin V binding was measured via flow cytometry. With 72 hours of CPI-766 exposure, some PARP cleavage was observed (Fig. 3-3a). Furthermore, 72 hours of DAC treatment followed by vehicle mock or CPI-203 induces a small amount of PARP cleavage, but exposure to CPI-766 following DAC treatment resulted in a substantial increase in PARP cleavage. Next, Annexin-V binding was measured following 3 days of either DAC or mock treatment, followed by seven days of continual exposure to KDM5 inhibitors. Whereas no changes in binding were observed following exposure to the KDM5 inhibitors alone, addition of CPI-455 or CPI-766 following DAC treatment resulted in a significant increase in binding relative to DAC alone (Fig. 3-3b).

3.2.3 KDM5 inhibitors alone, or in combination with DAC, do not alter cell cycle

To assess if exposure to KDM5 inhibitors, either alone or in combination with DAC, could alter cell cycle, we quantified total cellular DNA content via Propidium Iodide staining followed by flow cytometry. Following either three or five days of

continual KDM5 inhibitor exposure, after three days of incubation with DAC or mock treatment, no significant changes in cell cycle were observed (Fig. 3-4).

3.3 Discussion

Here we have shown that the KDM5 inhibitors and DAC synergistically inhibit proliferation in three luminal breast cancer cell lines. We observed varying degrees of synergy across the cell lines; in MCF-7 and T-47D the drug combination was moderately synergistic, whereas the degree of synergy was much higher in EFM-19. The mechanism for this difference is unclear, but given that the IC_{50} values for each of the compounds alone was lower in EFM-19 than in the other two cell lines tested, this cell line may be more sensitive to epigenetic perturbations in general, or any chemotherapeutic intervention. Regardless, this synergistic interaction appears to be mediated by an increased induction of apoptosis, as significant increases in PARP cleavage and Annexin-V biding were detected. Interestingly, the KDM5 inhibitors did not induce significant alterations in the cell cycle, either alone or in combination with DAC.

Although this is currently the subject of intense investigation, the treatment of breast cancer with epigenetic therapy has so far, shown little clinical efficacy. The synergistic interaction between these two classes of therapeutic agents suggests that dual targeting of histone demethylation and DNA methylation pathways may represent a promising new avenue for the application of epigenetic therapy to the treatment of breast cancer. First, combination therapy mediated a reduction in the amount of DAC needed to achieve the same efficacy. Given the high toxicity of DAC treatment in human patients, this reduction in dose could be of critical translational importance. Furthermore, the synergistic interaction described above indicates that these epigenetic pathways exert independent effects on cancer cell growth, and targeting both pathways with combination treatment exerts a greater anti-proliferative effect than either drug alone. Although *in-*

vivo modeling was impossible in this study due to the low bioavailability of the KDM5 inhibitors, these data suggest that further development and refinement of these compounds could yield promising results in the treatment of breast cancer.

Finally, KDM5 inhibition, alone or in combination with DAC, may also prove useful in treating hormone resistant breast cancers. Although adjuvant hormonal therapy, most commonly with selective estrogen receptor modulators (SERMs) such as Tamoxifen, has greatly improved survival in patients with hormone receptor positive tumors, resistance to hormonal therapy represents a significant clinical burden. Recently, a study by Yamamoto et al. associated high KDM5B activity with decreased survival in patients with hormone resistant tumors (Yamamoto et al, 2014). This finding suggests that the KDM5 proteins, KDM5B in particular, may be critical drivers of the hormone resistant phenotype; chemical inhibition of the KDM5 proteins may represent a promising new avenue in the treatment of these tumors. Future studies should investigate these intriguing findings.

3.4 Materials and methods

3.4.1 KDM5 inhibitors

Two active KDM5 inhibitor compounds, CPI-455 and CPI-766, and one inactive control compound, CPI-203, were obtained from Constellation Pharmaceuticals. All compounds were dissolved in DMSO to a final concentration of 10 mM. Eluted drug was stored at -20°C.

3.4.2 Cell lines

MCF-7, T-47D, and EFM-19 are luminal breast cancer cells. MCF-7 was grown in MEM supplemented with 10% fetal bovine serum (FBS), T-47D and EFM-19 were grown in RPMI 1640 supplemented with 10% FBS. All cell lines were incubated at 37°C with a 5% CO_2 atmosphere.

3.4.3 Cytotoxicity assays after combination drug treatment

$3x10^4$ MCF-7 cells, $5x10^4$ T-47D cells, or $7.5x10^4$ EFM-19 cells were plated in 96-well cell culture plates and incubated overnight. The following day, the media was aspirated and replaced with DAC containing normal media at the indicated doses; in each experiment, each dose was repeated in three technical replicates. DAC media was replaced every 24 hours for a total treatment time of 72 hours. Following DAC treatment, DAC media was aspirated and replaced with KDM5 inhibitor containing media supplemented with 2% FBS. KDM5 inhibitor dose was held at a constant ratio of 150:1 relative to the respective DAC dose. Total percentage of DMSO (0.5%) was normalized across all treatment groups. Cells were treated with KDM5 inhibitors for 10

days; media was aspirated and replaced with fresh drug containing media on days 3 and 7.

Following treatment, total cell viability was measured with Promega CellTiteer AQueous Non-Radioactive Cell Proliferation Assay (MTS) (#G5421). Data shown represent the mean across three independent replicates.

3.4.4 Synergy Calculation

Combination Index values, Dose Reduction Index values, and Isobolograms were calculated in CompuSyn software. For Combination Indices, values <1 indicate synergy, values=1 indicate additivity, and values >1 indicate antagonism between the two drugs. Dose reduction indices represent the change in the amount of drug needed in combination in order to achieve the same effect level of the single drug.

3.4.5 PARP Cleavage & Western Blotting

For each treatment condition, $2.5x10^5$ MCF-7 cells were plated in T25 flask and allowed to rest overnight. The following day, the media was aspirated and replaced with media containing DAC at a final concentration of 62.5 nM. DAC media was aspirated and replaced every 24 hours for a total treatment time of 72 hours. Following DAC treatment, media was aspirated and replaced with media supplemented with 2% FBS containing KDM5 inhibitors at a final concentration of 9.375 uM. Cells were harvested at the times indicated. Media was aspirated and replaced with fresh drug containing media on days 3 and 7.

Cell pellets were lysed in 4% SDS and the lysate was homogenized using Qiashredder columns (Qiagen #79656). Protein content was quantified using bicinchoninic acid (BCA) protein assay (Thermo #23225). Western blotting was performed as previously described (Cai et al. 2014)

The following primary antibodies were used: anti-cleaved PARP (Cell Signaling #9542) and anti-beta actin (Sigma #A2547). The following secondary antibodies were used: anti-Mouse IgG-HRP (GE #NA931V) and anti-Rabbit IgG-HRP (GE #NA934V).

3.4.6 Flow Cytometry

For each treatment condition, $2.5x10^5$ MCF-7 cells were plated in T25 flask and allowed to rest overnight. The following day, the media was aspirated and replaced with media containing DAC at a final concentration of 62.5 nM. DAC media was aspirated and replaced every 24 hours for a total treatment time of 72 hours. Following DAC treatment, media was aspirated and replaced with media supplemented with 2% FBS containing KDM5 inhibitors at a final concentration of 9.375 uM. Cells were harvested at the times indicated. Media was aspirated and replaced with fresh drug containing media on days 3 and 7.

To study apoptosis, $2x10^5$ cells were harvested at the indicated times and washed twice with cold PBS and then stained with Annexin V-FITC and Propidium Iodide (BD #556547) according to manufacturer's protocol. Cells were analyzed on a FACSCalibur flow cytometer with FlowJo software. To study cell cycle, $2x10^5$ cells were harveste at the indicated times, washed twice with PBS, and then fixed in 70% ethanol overnight at -20°C. Ethanol was then aspirated, washed once with PBS, and then stained with

Propidium Iodide (0.05 mg/mL final conc) (Sigma #P4864) and RNase A (0.1 mg/mL final conc) (Thermo #EN0531) containing buffer. Cells were analyzed on a FACSCalibur flow cytometer with FlowJo software.

3.4.7 Statistical Analysis

IC_{50} values, F scores, and p-values were calculated in GraphPad Prism 6 software using a variable slope (four parameter) non-linear fit. Error bars shown represent the standard error of the mean (SEM) across three independent replicates.

Statistical analyses in flow cytometry experiments were done with Graphpad Prism 6 software. P-values indicate the result of a pairwise comparison using Fisher's exact test in a 2x2 contingency table.

3.5 Figures: Chapter 3

3.5.1 Figure 3-1. Combination treatment dose response curves in luminal breast cancer cell lines

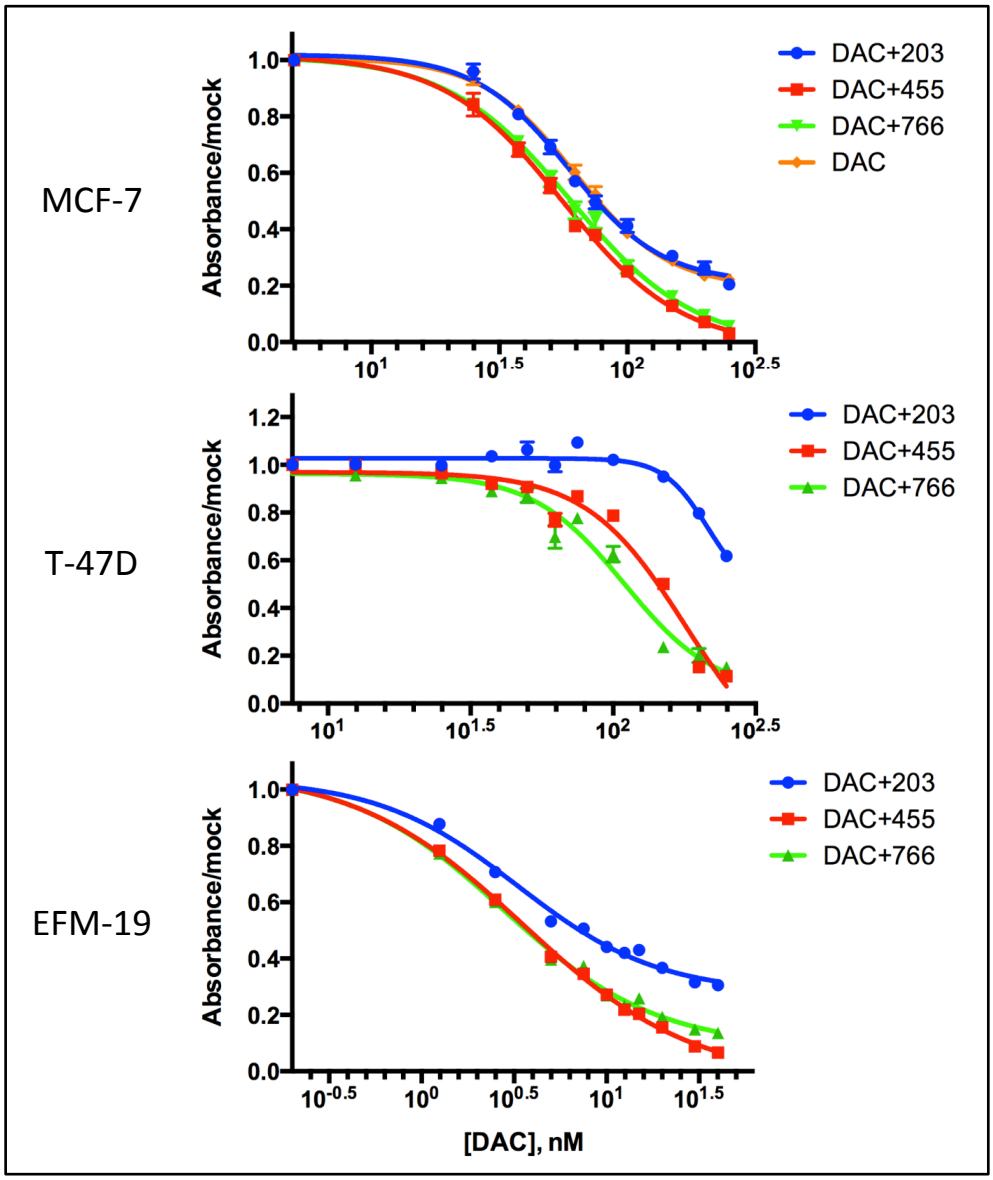

Figure 3-1. Cells were exposed to the indicated doses of DAC for 3 days, followed by 10 days of the indicated KDM5 inhibitor at a fixed dose ratio of 150:1 relative to DAC. Viability was measured as percent absorbance relative to mock treated samples using MTS assay.

3.5.2 Figure 3-2. KDM5 inhibitors synergize with DAC to inhibit cell proliferation.

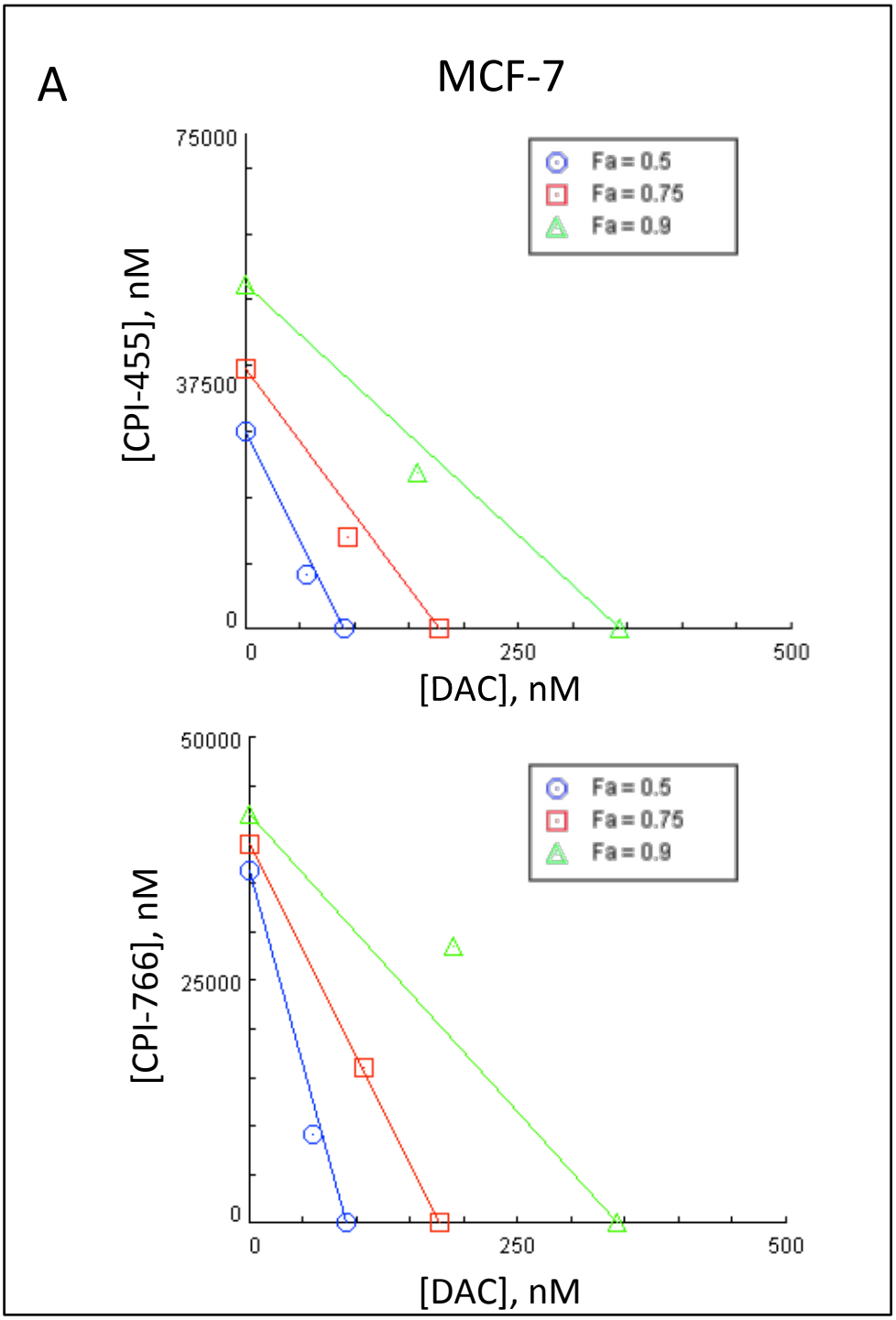

Figure 3-2a. Isobolograms for combination treatment with 72 hours of DAC and 10 days of KDM5 inhibitor in MCF-7.

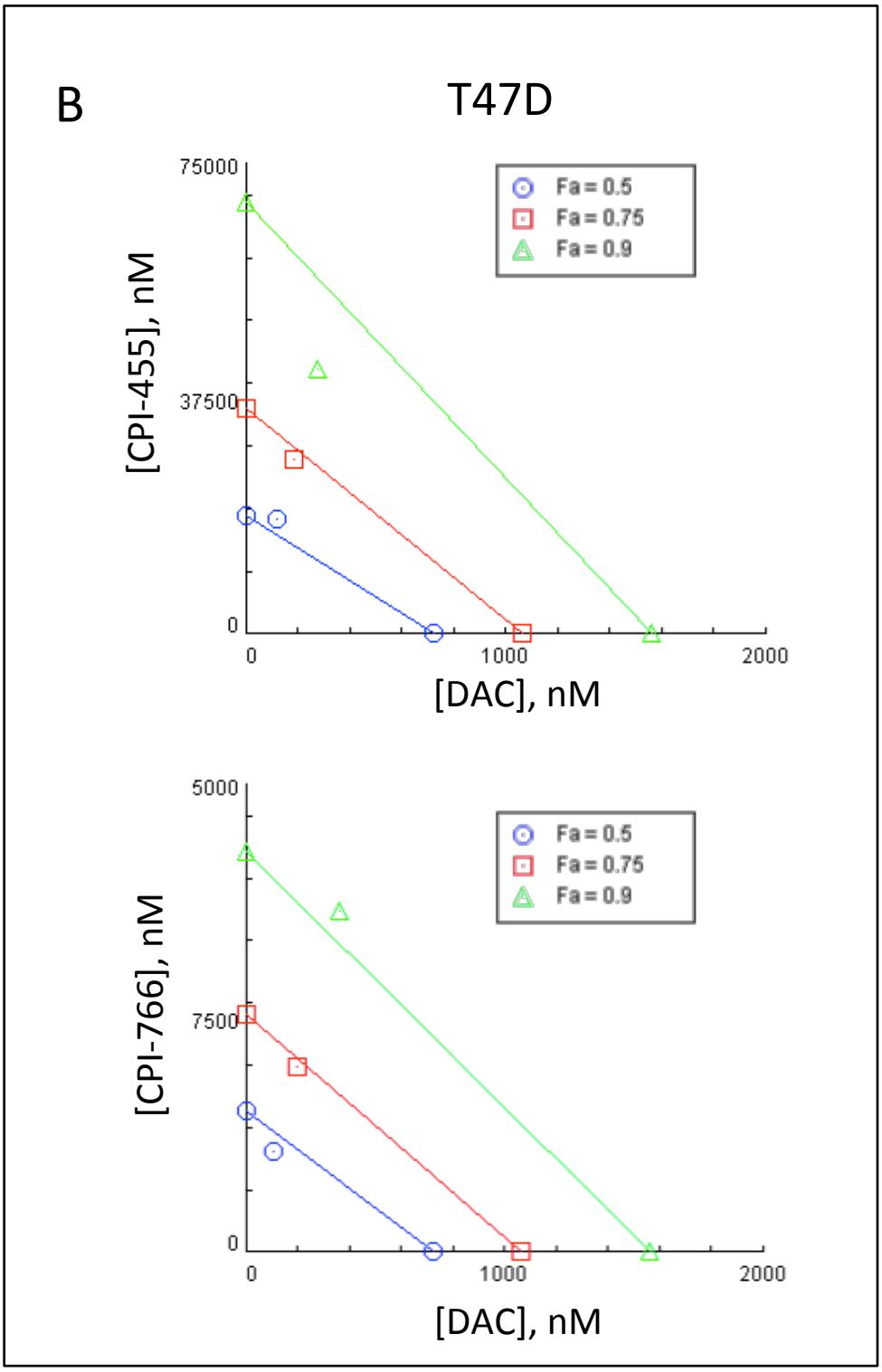

Figure 3-2b. Isobolograms for combination treatment with 72 hours of DAC and 10 days of KDM5 inhibitor in T-47D.

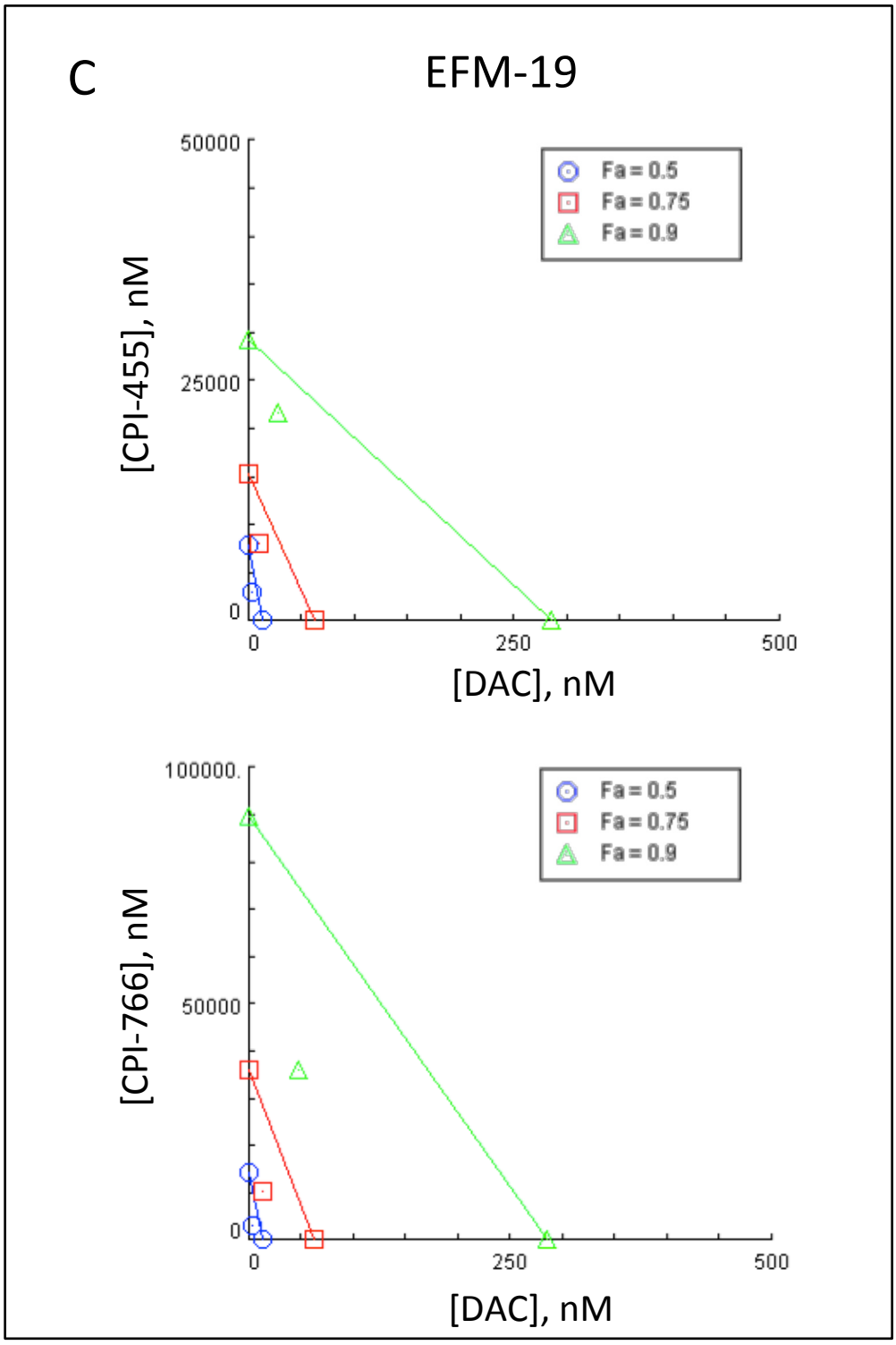

Figure 3-2c. Isobolograms for combination treatment with 72 hours of DAC and 10 days of KDM5 inhibitor in EFM-19.

3.5.3 Figure 3-3. Combination treatment increases apoptosis induction.

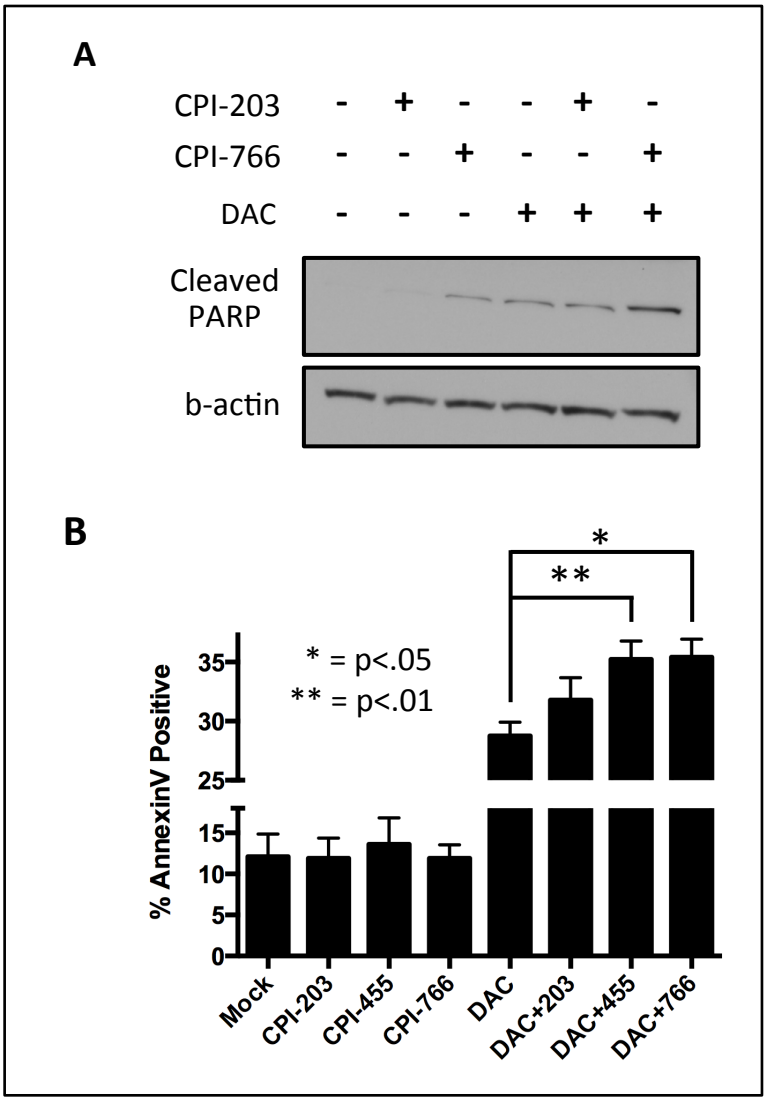

Figure 3-3. A. MCF-7 cells were either exposed to 62.5 nM DAC or mock control for 72 hours, then subsequently exposed to 9.375 uM of the indicated KDM5 for an additional 72 hours. PARP cleavage was assessed via immunoblot. Beta-actin was used as a loading control. B. MCF-7 cells were either exposed to 62.5 nM DAC or mock control for 72 hours, then subsequently exposed to 9.375 uM of the indicated KDM5 for an additional 7 days. Annexin V binding was measured via flow-cytometry. Error bars represent the SEM from 3 independent experiments.

3.5.4 Figure 3-4. Combination treatment does not alter cell cycle progression.

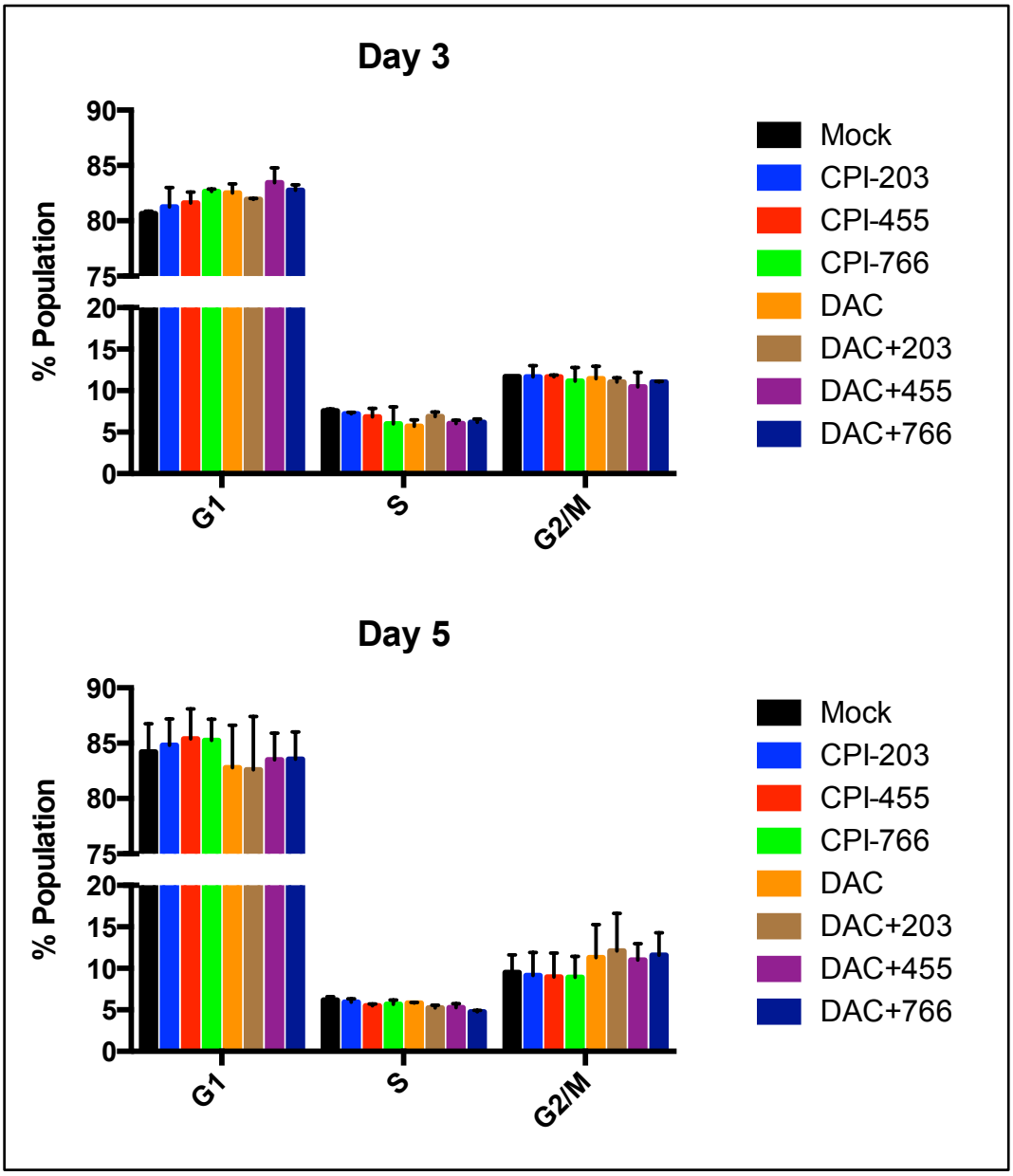

Figure 3-4. MCF-7 cells were either exposed to 62.5 nM DAC or mock control for 72 hours, then subsequently exposed to 9.375 uM of the indicated KDM5 for an additional 3 or 5 days. Cell cycle stage was assessed using propidium iodine staining followed by flow cytometry.

3.6 Tables: Chapter 3

3.6.1 Table 3-1. Combination Index (CI) values for DAC+KDM5 inhibitor treatments in 3 luminal breast cancer cell lines.

	DAC+455			DAC+766		
	MCF-7	T-47D	EFM-19	MCF-7	T-47D	EFM-19
Dose 1	0.94	6.12	0.79	0.87	0.41	0.67
Dose 2	0.88	1.53	0.64	0.87	0.73	0.5
Dose 3	0.89	1.4	0.59	0.87	0.77	0.39
Dose 4	0.83	1.69	0.71	0.88	0.95	0.52
Dose 5	0.94	1.15	0.71	1.00	0.73	0.41
Dose 6	0.94	2.03	0.71	0.98	1.05	0.42
Dose 7	0.98	1.95	0.8	1.17	1.01	0.58
Dose 8	0.99	1.41	0.83	1.28	0.71	0.51
Dose 9	0.86	0.73	0.73	1.35	0.86	0.56
Dose 10	N/A	0.76	0.76	N/A	0.92	0.67

Table 3-1. CI values for combination of 72 hours of incubation with DAC followed by 10 days incubation with the indicated KDM5 inhibitor. Doses shown correspond to doses in Figure 3-1.

3.6.2 Table 3-2. Dose Reduction Index (DRI) Values for DAC+KDM5 inhibitor treatments in 3 luminal breast cancer cell lines.

	DAC+455			DAC+766		
	MCF-7	T-47D	EFM-19	MCF-7	T-47D	EFM-19
Dose 1	1.34	5.06	1.88	1.32	19.43	2.03
Dose 2	1.54	8.97	2.99	1.42	10.56	3.14
Dose 3	1.60	8.11	4.64	1.52	9.20	4.91
Dose 4	1.82	6.46	4.42	1.59	7.34	3.75
Dose 5	1.64	7.54	5.38	1.44	8.60	5.44
Dose 6	1.77	4.96	6.38	1.69	6.19	5.69
Dose 7	1.93	4.56	6.02	1.64	6.01	3.92
Dose 8	2.15	4.80	7.09	1.76	7.27	4.96
Dose 9	2.94	6.60	11.50	2.01	5.87	5.06
Dose 10	N/A	5.93	13.29	N/A	5.29	4.40

Table 3-2. DRI values for combination of 72 hours of incubation with DAC followed by 10 days incubation with the indicated KDM5 inhibitor. Doses shown correspond to doses in Figure 3-1.

4. CHAPTER 4: MOLECULAR EFFECTS OF COMBINATION TREATMENT WITH 5-AZA-2'-DEOXYCYTIDINE AND KDM5 INHIBITORS IN A LUMINAL BREAST CANCER CELL LINE

4.1 Introduction

As described in Chapter 1, epigenetic modifications of DNA and histones play an essential role in transcriptional regulation. At more than half of the genes in the genome, promoter regions contain CpG rich regions called CpG islands; methylation of these islands is associated with transcriptional silencing (Bird 2002). However, almost 90% of these promoter CpG islands remain free from DNA methylation throughout development and adult life (Suzuki et al. 2008). These regions are, then, among the many transcription start sites of active genes that are characterized by having a central a nucleosome-depleted region that is flanked by enrichment for histone 3 lysine 4 trimethylation (H3K4me3). However, in cancers of virtually all types, 5 to 10% of these promoters, some involving classic tumor suppressor genes, can accrue abnormal, de novo, DNA methylation during tumor progression (Baylin & Herman 2000). Perhaps not surprisingly, when the epigenetic modifiers responsible for regulating these phenomena are perturbed, either through chemical or genetic manipulation, global molecular changes can be produced. Inhibition of the DNA methylation machinery by DNA demethylating agents, such as AZA or DAC, induces substantial alterations in gene expression patterns and these changes are mediated by global loss of DNA methylation (Scheubel et al. 2007). These agents, as noted in earlier chapters, are utilized as therapeutic agents with one hypothesis being that their treatment efficacy can be associated with re-expression of the abnormally DNA methylated genes noted above (Tsai et al. 2011). Furthermore,

these losses of promoter DNA methylation are accompanied by a massive reorganization of the chromatin architecture, with most target promoters losing repressive histone modifications (McGarvey et al. 2008, Komashko & Farnham, 2010). Perturbations to maintenance of H3K4 methylation equilibrium however, are far less well understood. One of the first studies of KDM5B noted the vital role of this protein as a transcriptional repressor, as stable knockdown of this protein resulted in the upregulation of a number of genes (Yamane et al. 2007). Recently, a global analysis of the effects of KDM5B reduction in breast cancer cells via siRNA found that, although loss of this protein was associated with dramatic lineage associated expression changes, the absolute number of genes with differential expression patterns were relatively small (Yamamoto et al. 2014). These authors proposed that, KDM5B is not a master regulator of transcription, but rather a fine-tune modifier capable of specifying lineage dependent gene expression patterns.

Given these observations, we next sought to characterize the molecular changes associated with the synergistic inhibition of proliferation mediated by combination treatment with DAC and the KDM5 inhibitors. Using the luminal breast cancer cell line MCF-7 as a model, we first characterized global gene expression changes mediated by the KDM5 inhibitors, either alone or in combination with DAC, using the Agilent 4x44k v2 microarray. Next, we analyzed whole genome changes to DNA methylation via the Illumina Infinium HumanMethylation450 microarray. Finally, we measured changes in H3K4me3 and KDM5B localization via chromatin immunoprecipitation (ChIP) followed by quantitative-PCR (qPCR). We hypothesized that, similar to reduction of KDM5B levels via siRNA, administration of the KDM5 inhibitors alone would mediate the differential expression of a number of genes. Furthermore, given the synergy between

DAC and the KDM5 inhibitors discussed in the previous chapter, we hypothesized that the addition of KDM5 inhibitors to DAC treated cells would further alter gene expression patterns relative to DAC alone. We were also interested in determining the mechanism of these gene expression pattern alterations; specifically, could the KDM5 inhibitors facilitate a further reduction in DNA methylation? This might ensue because studies have well outlined that this active histone mark is antagonistic to de novo placement of DNA methylation (Ooi et al. 2007). Conversely, DNA methylation could be unaffected by KDM5 inhibition after DAC treatment, and expression changes were mediated by alterations to the localization patterns of the KDM5 histone substrate, H3K4me3. Here, we aim to answer these questions via an integrated analysis of the molecular effects of KDM5 inhibitor treatment, either alone or in combination with DAC.

4.2 Results

4.2.1 KDM5 inhibitor, either alone or in combination with DAC, result in significant differential gene expression

Whole genome expression patterns were assessed in MCF-7 cells following exposure to one of our KDM5 inhibitor compounds, DAC, or a combination of the two. Gene expression patterns from three independent drug treatments were measured using the Agilent 4x44k Human v2 microarray; the expression value for each probe was determined by using the median intensity value across the three replicates. To assess the expression changes specifically mediated by KDM5 inhibition, intensity values for the active KDM5 inhibitors were normalized relative to the inactive compound; similarly, intensity values for cells exposed to DAC and one of the active KDM5 inhibitors were normalized relative to cells exposed to DAC and the inactive KDM5 inhibitor. Any probes with an adjusted p-value <0.05 were deemed to indicated significant differential expression relative to the control sample.

We found that exposure to either of the two active KDM5 inhibitors, CPI-455 or CPI-766, induces significant differential gene expression at target loci relative to the inactive compound CPI-203. Specifically, exposure to CPI-455 results in the differential expression of 234 transcripts corresponding to 169 unique genes (Fig. 4-1a, Table 4-1). Exposure to CPI-766 resulted in the differential expression of a substantially larger group of loci; 980 transcripts corresponding to 646 unique genes were significantly differentially expressed (Fig. 4-1a, Table 4-1). The two drugs appear to regulate similar targets, as a significant degree of overlap (Chi-square test with Yate's correction, $p<0.0001$) between the two differentially expressed gene sets was detected (Fig 4-1b).

To further illustrate the effect that these active KDM5 inhibitors on gene expression, we determined which transcripts were significantly differentially expressed in both CPI-455 and CPI-766 treated samples relative to the treatment mock sample. We then generated a heatmap from the 500 most significantly differentially expressed transcripts to compare expression values between these samples and the inactive compound, CPI-203. Though CPI-203 did affect transcription at some of these loci, we found that most of these targets are unaffected by exposure to CPI-203 (Fig. 4-3). Interestingly, a number of these targets are also differentially expressed following DAC treatment, though many appear to be targets specific to the KDM5 inhibitors (Fig. 4-3).

Similarly, the addition of either of the two active KDM5 inhibitors following exposure to DAC resulted in significant differential gene expression relative to DAC followed by CPI-203. We found that DAC followed by CPI-455 resulted in the differential expression of 84 different transcripts corresponding to 57 unique genes, and DAC followed by CPI-766 resulted in the differential expression of 480 transcripts corresponding to 331 unique genes relative to DAC followed by CPI-203 (Fig. 4-2a, Table 4-1). Again, there was a significant degree of overlap between the genes differentially expressed by DAC+455 and DAC+766 (Chi-square test with Yate's correction, $p<0.0001$), indicating that that these compounds act on similar targets (Fig. 4-2b). To further illustrate the effect of the active KDM5 inhibitors in combination with DAC, we determined which transcripts were significantly differentially expressed after both DAC+455 and DAC+766 treatment of samples relative to DAC alone. Using these loci, we then generated a heatmap to compare expression values from these samples to those of samples treated with DAC+203. We found that, for most of these transcripts, the

addition of the inactive compound, CPI-203, following DAC treatment had no effect on the expression (Fig. 4-4).

Next, we sought to further characterize the genes differentially expressed following exposure to the KDM5 inhibitors. First, we assessed the basal expression levels of genes with significant differential expression following KDM5 inhibitor treatment. We found that genes that are upregulated by exposure to the KDM5 inhibitors alone are relatively highly expressed, as the basal expression levels of these loci are well above the median expression values for all genes (Fig. 4-5). Similarly, the basal expression rates for genes that were upregulated by the addition of the KDM5 inhibitors following DAC treatment were substantially higher than the median expression rate for all genes.

To determine if chemical inhibition of the KDM5 proteins induced gene expression patterns similar to those induced by reduction of the protein levels, we compared our data to the genes that were differentially expressed following siRNA mediated knockdown of KDM5B in MCF7, as described in a recent study by Yamamoto et al., using Gene Set Enrichment Analysis software (GSEA) (Yamamoto et al, 2014). We found that genes upregulated following treatment with KDM5 inhibitors alone were significantly enriched for genes that were also upregulated following KDM5B knockdown. Similarly, genes upregulated following treatment with DAC+455 or DAC+766 relative to the inactive combination were also significantly enriched for genes upregulated following KDM5B knockdown (Fig. 4-6a) (Yamamoto et al. 2014).

Furthermore, we were interested in assessing how the gene expression patterns observed here correlate with previously observed patterns following other perturbations

to epigenetic modifiers. Using GSEA to probe genes upregulated following either KDM5 inhibitor treatment alone, or in combination with DAC, we found significant enrichment for genes upregulated following knockdown of the H3K4 demethylase KDM1 (LSD1), as well as genes upregulated following knockdown of Polycomb Repressive Complex 2 (PRC2) member, SUZ12 (Fig. 4-6b) (Pasini et al. 2007, Wang et al. 2007). Similarly, in both of our treatment groups, we observed significant enrichment for targets upregulated following combination treatment with DAC and the histone deacetylase class 1 and II inhibitor, trichostatin A (Fig. 4-6b) (Heller et al. 2008).

Next, we determined the effects of the KDM5 inhibitors on immune regulation signaling pathways. A recent study observed that a number immune related signaling pathways that are normally lowly expressed in cancer, presumably to aid immune evasion, are significantly upregulated following treatment with the DNA hypomethylating agent, 5-azacytidine (AZA) (Li et al. 2014). To determine if KDM5 inhibition, either alone or in combination with DAC, we created gene sets for chemokine/cytokine signaling, inflammation, and viral defense based on the gene pathways that were upregulated after AZA treatment in three different cancer types according to Li *et al.*, and queried them against our gene expression data using GSEA. We found that when administered alone, the KDM5 inhibitors significantly upregulate all three immune related pathways (Fig. 4-6c). Similarly, when compared to DAC+203, the addition of the active KDM5 inhibitors to DAC treatment resulted in the significant upregulation of these immune signaling pathways (Fig. 4-6c).

4.2.2 DNA methylation unaffected by KDM5 inhibitor treatment

Given the changes in gene expression observed following treatment with either of the KDM5 inhibitors, either alone or in combination with DAC, we next determined if these changes were associated with a reduction in DNA methylation levels. Here, we utilized the Illumina Infinium HumanMethylation450 microarray to measure methylation levels at 450 thousand unique loci throughout the genome. Upon assessing methylation levels at all probes throughout the genome, administration of either CPI-455 or CPI-766 did not lead to a reduction in DNA methylation (Fig. 4-7). Not surprisingly, a reduction in global DNA methylation was observed in all DAC treated samples, with a slightly greater level of demethylation observed in cells treated with DAC and CPI-766 (Fig. 4-7). Similar patterns were observed when measuring methylation at CpG island, CpG shore, and gene body probes (Fig. 4-7).

Although no drastic reductions in global levels of DNA methylation were observed following treatment with the KDM5 inhibitors, we next tested if these compounds could mediate local changes at the promoters of the differentially expressed loci as a result of KDM5 inhibition. First, we determined if the promoter, CpG island regions of loci that were significantly upregulated following KDM5 inhibitor treatment, either alone or in combination with DAC, were basally methylated in the MCF-7 mock treatment group. Any gene containing a CpG island probe within a range of -500 bp to +1500 bp from the transcription start site (TSS) that had a beta value ≥ 0.75 was deemed to be methylated. We found that a substantial number of genes upregulated by either CPI-455 or CPI-766 alone contained basal methylation in their promoters (18.9% of genes up after CPI-455, 19.2% of genes up after CPI-766) (Fig. 4-8). Similarly, many genes upregulated after DAC+455 and DAC+766 treatments contained basal methylation

(20.4% of genes up after DAC+455, 22.7% of genes up after DAC+766) (Fig. 4-8). Given our previous finding that genes differentially expressed after KDM5 inhibition possessed relatively high basal transcription rates, we next probed the basal expression specifically at these methylated loci. When compared to the expression levels of all methylated loci in the genome, we found that methylated genes that were significantly upregulated following KDM5 inhibition alone were transcribed at a significantly higher rate basally (Mann-Whitney U test, $p<0.0001$) (Fig-9). Similarly, methylated genes upregulated by KDM5 inhibition following DAC treatment possessed basal transcription rates significantly higher than the other methylated loci (Mann-Whitney U test, $p<0.0001$) (Fig. 4-9).

Finally, to test if KDM5 inhibition directly mediated loss of methylation at upregulated loci, we compared the change in methylation beta values at CpG island TSS probes for each of the drug treatments relative to the treatment mock or DAC treated samples. When normalized to the mock treatment, treatment with either CPI-455 or CPI-766 alone did not result in substantial methylation changes when compared to CPI-203 and almost no changes in methylation were observed at significantly upregulated loci (Fig. 4-10). We next conducted the same analysis on samples exposed to the KDM5 inhibitors following DAC treatment. When normalized to the mock treatment, substantial loss of methylation is observed at CpG island TSS loci in all samples exposed to DAC, including loci found at the promoters of targets significantly upregulated by the addition of KDM5 inhibitors (Fig. 4-11). But, when normalized to the DAC treated sample, it is apparent that KDM5 inhibition does not mediate further demethylation of these upregulated genes (Fig. 4-11).

4.2.3 KDM5 inhibitor treatment enhances H3K4me3 levels at target promoters

With these findings in mind, we next determined if the previously observed changes in gene expression were associated with altered promoter levels of H3K4me3, perhaps mediated by a loss of KDM5 catalytic function at these loci. First, we determined if KDM5B was enriched within the promoters of a panel of genes that were significantly upregulated either by KDM5 inhibitor treatment alone or in combination with DAC. Using chromatin immunoprecipitation (ChIP), followed by quantitative PCR (qPCR), we found that KDM5B was significantly enriched within the promoters of *APOE*, *ANXA1*, *PLEKHG4*, and *SNAI1* (Fig 4-12a). Next, given that these four genes were significantly upregulated and enriched for KDM5B, we determined if KDM5 inhibitor treatment lead to an increase in H3K4me3 within these promoters. Whereas treatment with inactive compound alone lead to no changes in H3K4me3 levels, treatment with the two active KDM5 inhibitors alone lead to a 1.5-4 fold increase in H3K4me3 enrichment at these promoters relative to mock. Furthermore, combination treatment with DAC and the KDM5 inhibitors resulted in an even greater increase in H3K4me3 levels (Fig. 4-12b). Surprisingly, no changes in H3K4me3 enrichment relative to mock were observed after treatment with DAC alone, or in combination with the inactive KDM5 inhibitor, CPI-203 (Fig. 4-12b).

Next, we sought to determine the extent to which increases in H3K4me3 were associated with upregulation of gene expression at these loci. We found that at 3 out of 4 of the loci tested (*APOE, ANXA1,* and *PLEKHG4*), increases in expression were associated with significant increases H3K4me3 enrichment relative to mock (Fig. 4-12b-c). Increases in expression at all 4 loci were also observed in DAC alone and DAC+203

treated samples (Fig. 4-12b-c), despite no significant changes in H3K4me3 enrichment, potentially indicating that these loci are upregulated through an independent mechanism after DAC treatment. The combination of active KDM5 inhibitors and DAC resulted in the greatest increases in H3K4me3 levels as well as the greatest upregulation of gene expression (Fig. 4-12b-c).

4.3 Discussion

Here, we have demonstrated that treatment with the KDM5 inhibitors results in significantly altered gene expression patterns and can enhance the molecular effects of DAC. Administration of these compounds alone results in the significant differential expression of hundreds of distinct loci. Interestingly, incubating cells with the KDM5 inhibitors after 72 hours of DAC exposure also mediated significant differential expression relative to DAC alone or DAC plus the inactive compound, CPI-203. The basal expression rates of genes in parental MCF-7 significantly upregulated by KDM5 inhibitor treatment were relatively highly expressed compared to all genes in the genome. Although counter-intuitive, this finding is in agreement with a recent study that observed KDM5B localization to highly active gene promoters (Yamamoto et al. 2014). These findings indicate that the KDM5 proteins are likely not master repressors of transcription, but rather they act as fine tune transcriptional regulators, likely as part of a repressive complex that is functionally balanced by complementary transcriptional activators. Regardless these data demonstrate that when administered together, much like the synergistic inhibition of growth described in the previous chapter, the KDM5 inhibitors and DAC exert at least additive effects on the cell.

We were next interested in comparing the molecular effects of our KDM5 inhibitors to those of other epigenetic perturbations. First, when queried against gene expression patterns after KDM5 inhibitor treatment, we found significant enrichment for genes upregulated by knockdown of KDM5B, indicating that inhibition of catalytic activity is sufficient for the upregulation of many KDM5B targets. Next, we compared our gene expression patterns to those of various other epigenetic perturbations including

genes upregulated by combination treatment with DAC and TSA and genes upregulated after knockdown of either LSD1 or the PRC2 member, SUZ12. We found significant, positive enrichment in each of these gene sets. These observations indicate that many of these targets are subject to various modes of epigenetic regulation, and perturbations to just one of these epigenetic modifiers is sufficient to increase expression at these loci. Finally, given that a recent study out of our group demonstrated the significant upregulation of lowly expressed immune regulatory pathways, or AZA immune genes (AIM), we next determined if KDM5 inhibition, either alone or in combination, exerted a similar stimulatory effect. We found that, not only could the KDM5 inhibitors upregulate AIM pathways, but the KDM5 inhibitors could also enhance the effects of DAC on these pathways. Although these findings were not functionally validated here, these intriguing observations suggest that KDM5 inhibition could mediate an increased susceptibility to immune attack *in-vivo*. Furthermore, combination treatment with DAC and the KMD5 inhibitors could enhance immune priming and increase susceptibility to immune checkpoint therapeutic agents such as anti-PD1/PDL1 or anti-CTLA4 antibodies. These hypotheses could prove to be of great translational relevance, and should be addressed in future studies.

We next sought to determine the mechanism by which the KDM5 inhibitors affected gene expression. We proposed two alternate hypotheses; first, that KDM5 inhibition would increase H3K4me3 levels at target loci and this increase would directly mediate increased transcription. Second, in cells exposed to the combination of KDM5 inhibitors and DAC, this increase in H3K4 methylation could possibly mediate an enhancement of DNA demethylation. In regards to the latter hypothesis, we assessed

global DNA methylation and found that treatment with the KDM5 inhibitors did not produce notable alterations either in global levels of DNA methylation level, or within the promoters of differentially expressed genes. Similarly, the addition of CPI-766 to DAC treatment resulted in a slightly greater loss of global DNA methylation, but no change in promoter methylation was observed at differentially expressed loci. From this, we concluded that the gene upregulation we observed in the combination treatment was not due to an enhancement of DNA demethylation. Next, given that catalytic inhibition of KDM5 proteins should mediate an increase in H3K4me3, we measured levels of this mark at the promoters of differentially expressed, KDM5B target genes. We observed a 1.5-4 fold increase in H3K4me3 levels from incubation with the KDM5 inhibitors alone, and an even greater increase from the combination treatment with DAC and the KDM5 inhibitors. Surprisingly, no significant changes in H3K4me3 levels were found at these promoters in cells exposed to either DAC or DAC+203. Despite this observation, expression at these loci is upregulated following treatment with DAC or DAC+203, indicating that a different epigenetic mechanism is responsible for the repression at these loci. Given that *APOE, ANXA1,* and *SNAI1* contain no DNA methylation within their promoters, perhaps DAC administration mediates a loss of repressive histone methylation marks, as observed in previous studies (Komashko & Farnham, 2010). Nevertheless, increases in local levels of H3K4me3 mediated by inhibition of the KDM5 proteins is associated with increases in transcription; indicating that loss of H3K4 methylation is at least partially responsible for the repression of these loci. Furthermore, as indicated by the greater induction of expression after treatment with the combination of DAC and KDM5 inhibitors, such a treatment protocol is likely targeting distinct epigenetic

mechanisms that function together in the regulation of gene expression, thereby resulting in the additive gene upregulation observed here. Future studies should test this hypothesis and address the extent to which levels of repressive chromatin marks are altered by the combination of DAC and KDM5 inhibitors.

4.4 Materials and methods

4.4.1 KDM5 Inhibitors

Two active KDM5 inhibitor compounds, CPI-455 and CPI-766, and one inactive control compound, CPI-203, were obtained from Constellation Pharmaceuticals. All compounds were dissolved in DMSO to a final concentration of 10 mM. Eluted drug was stored at -20°C.

4.4.2 Cell lines

MCF-7 is a luminal breast cancer cell line. MCF-7 was grown in MEM supplemented with 10% fetal bovine serum (FBS) and was incubated at 37°C with a 5% CO_2 atmosphere.

4.4.3 Combination Drug Treatment

For each treatment condition, $2.5x10^5$ MCF-7 cells were plated in T25 flask and allowed to rest overnight. The following day, the media was aspirated and replaced with media containing DAC at a final concentration of 62.5 nM. DAC media was aspirated and replaced every 24 hours for a total treatment time of 72 hours. Following DAC treatment, media was aspirated and replaced with media supplemented with 2% FBS containing KDM5 inhibitors at a final concentration of 9.375 uM. Cells were harvested following 72 hours of KDM5 inhibitor treatment.

4.4.4 Analysis of Gene Expression

Total RNA from MCF-7 cells treated according to the combination treatment protocol (described previously in this chapter) was extracted using Qiagen RNeasy RNA extraction kit (#74104) and then further purified using a standard isopropanol precipitation method previously described (Cathala *et al*. 1983). For each treatment group, whole genome expression analysis was assayed on the Agilent Human 4x44k v2 expression array. Three independent replicates for each treatment group were submitted for expression analysis.

Analysis of whole genome expression data was conducted in R software (www.R-project.org) using the Limma package (http://www.bioconductor.org/packages/release/bioc/html/limma.html). Expression data within each array was normalized using the Loess method and normalized between arrays using the aquantile method and subsequently transformed to log2 scale. Differential expression relative to the inactive compound (CPI-203) either alone or in combination with DAC, was calculated for each probe was determined using linear model generated by the *lmfit()* command. Statistics for differential expression were generated using the *ebayes()* command. P-values were corrected for multiple testing using the bonferoni-hochberg method. All probes with a corrected p-value <0.05 were deemed to be significantly differentially expressed.

4.4.5 Analysis of DNA Methylation

Genomic DNA from MCF-7 cells treated according to the combination treatment protocol described previously in this chapter was extracted using the Promega Wizard Genomic DNA Purification Kit (#A1120). For each treatment group, whole genome

methylation was analyzed using the Illumina Infinium HumanMethylation 450 array. Data shown represent the result of one independent experiment.

Whole genome methylation analysis was conducted in R software using the minfi package (http://www.bioconductor.org/packages/release/bioc/html/minfi.html). Background normalization of array data was conducted using the *preprocessIllumina()* command, and then within array normalization was conducted using the *preprocessSWAN()* command. Methylation beta values were obtained using the *getBeta()* command. Only probes with detection p values <0.01 were retained.

4.4.6 ChIP

$2x10^6$ MCF-7 cells were seeded in 15cm dishes and allowed to incubate overnight at 37°C supplemented with 5% CO_2. Cells were treated with fresh DAC (or drug mock) containing MEM media plus 10% FBS for 3 days, with fresh drug media replaced every 24 hours, at a dose of 62.5 nM. Following DAC treatment, cells were incubated with one of the KDM5 inhibitors or treatment mock in MEM plus 2% FBS medium at a dose of 9.375 uM for 72 hours.

Following drug treatment, to crosslink proteins, cells were incubated in 1% formaldehyde for 10 minutes at room temperature. The crosslinking reaction was stopped with glycine at a final concentration of 0.125 M. Cells were then scraped, harvested, and washed with twice PBS containing a protease inhibitor cocktail. Nuclear lysates were obtained as previous described (O'Hagan et al. 2011). Nuclear lysate were then sonicated using Diagenode water bath sonicator; sonication protocol consisted of 7 cycles of 30 seconds of sonication followed by 30 seconds of no sonication. Sonicated

nuclear lysate was then centrifuged at 20,000 x g for 10 minutes at room temperature. Supernatant was then transferred to a clean tube. 80ug of chromatin, 400 uL of SDS lysis buffer, and 3.6 mL of ChIP dilution buffer were added to each immunoprecipitation. The following antibodies were used: anti-H3 (Abcam, ab1791), anti-KDM5b (Novus Biologicals, #22260002), anti-H3K4me3 (Millipore #07-473**)**, and normal rabbit IgG (Millipore, #12-370). Antibodies were incubated with sonicated lysate on rotator at 4°C overnight. 100 uL of blocked magnetic Protein A and Protein G beads (mixed at 3:1 ratio), were then added to lysate and incubated with rotation for 3 hours at 4°C. Beads were then washed 6 times with ChIP wash buffers previous described (O'Hagan et, 2011). Crosslinking was then reversed via incubation at 65°C overnight.

De-crosslinked ChIP samples were then incubated with 2 uL RNAse A (20 mg/mL) for 1 hour at 37°C, and then incubated with 4 uL Proteinase K (10 mg/mL) for 2 hours at 55°C. DNA was then purified using Qiagen PCR purification kit.

Relative target enrichment was determined via quantitavive-PCR (qPCR). Reactions contained Bio-Rad iTaq Universal SYBR Green (#172-5120), specific primers, cDNA, and water. All reaction were run on ABI StepOnePlus real-time PCR system. Relative quantitation of each target was calculated as enrichment relative to input. Primer sequences are listed in Appendix 1.

4.4.7 Statistical Analysis

Volcano plots were generated in R software using log2 fold change on the x-axis and –log10 transformed corrected p-values on the y-axis calculated using three independent experimental replicates. The horizontal blue line indicates a corrected p-

value ≤ 0.05, and the vertical blue lines indicate a log2 fold-change ≥ ± 0.5. Each dot represents one probe.

Expression heatmaps were generated in R software using the gplots package and *heatmap.2()* command. Briefly, linear models were generated using methods described above to determine probes differentially expressed in cells treated with the active KDM5 inhibitors (alone or in combination with DAC) relative to cells treated with the inactive KDM5 inhibitor (alone or in combination with DAC). Heatmaps were plotted using log2 fold change relative to the respective control used in each figure.

Boxplots were generated in R software; the horizontal line inside the box indicates the median value and the 25th and 75th percentiles define the lower and upper limits of the box, respectively. Statistical significance tested using an unpaired T test. Venn diagrams were also generated in R software using the *overlapper()* command (http://faculty.ucr.edu/~tgirke/Documents/R_BioCond/My_R_Scripts/overLapper.R).

Gene set enrichment analysis was conducted using the pre-ranked list function in GSEA software (http://www.broadinstitute.org/gsea). Briefly, the log2 fold change value for each gene was calculated across three independent replicates by aggregating probes according to their respective gene and taking the median value. Genes were then sorted according to median log2 fold change values. These lists were then queried against he Molecular Signatures Database curated by the Broad Institute. For comparisons to the genes up-regulated in Yamamoto et al (2014), an additional gene set was constructed using the top up-regulated targets described in that paper.

Beta and delta beta scatter plots were generated in R software. Each dot represents one probe; red dots indicate probes corresponding to genes that are

significantly differentially expressed. For delta beta plots, the comparison used to generate delta beta values is indicated on each axis.

4.5 Figures: Chapter 4

4.5.1 Figure 4-1. Treatment with KDM5 inhibitors results in significant differential gene expression patterns

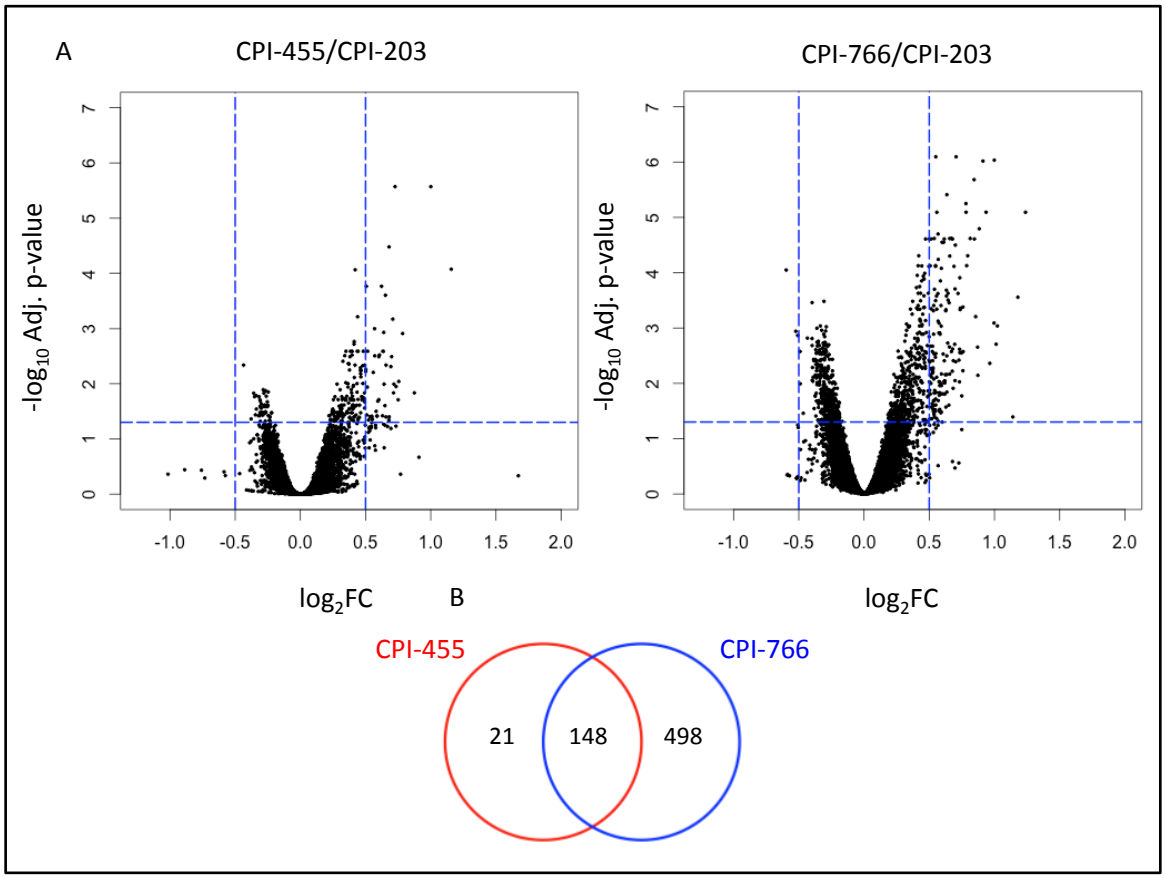

Figure 4-1. A. Volcano plots for gene expression changes for MCF-7 cells exposed to 9.375 uM KDM5 inhibitor for 72 hours relative to CPI-203. B. Venn diagram of overlap of differentially expressed genes following exposure to either active KDM5 inhibitor for 72hrs relative to CPI-203.

4.5.2 Figure 4-2. Combination treatment with active KDM5 inhibitors and DAC results in significant differential gene expression patterns

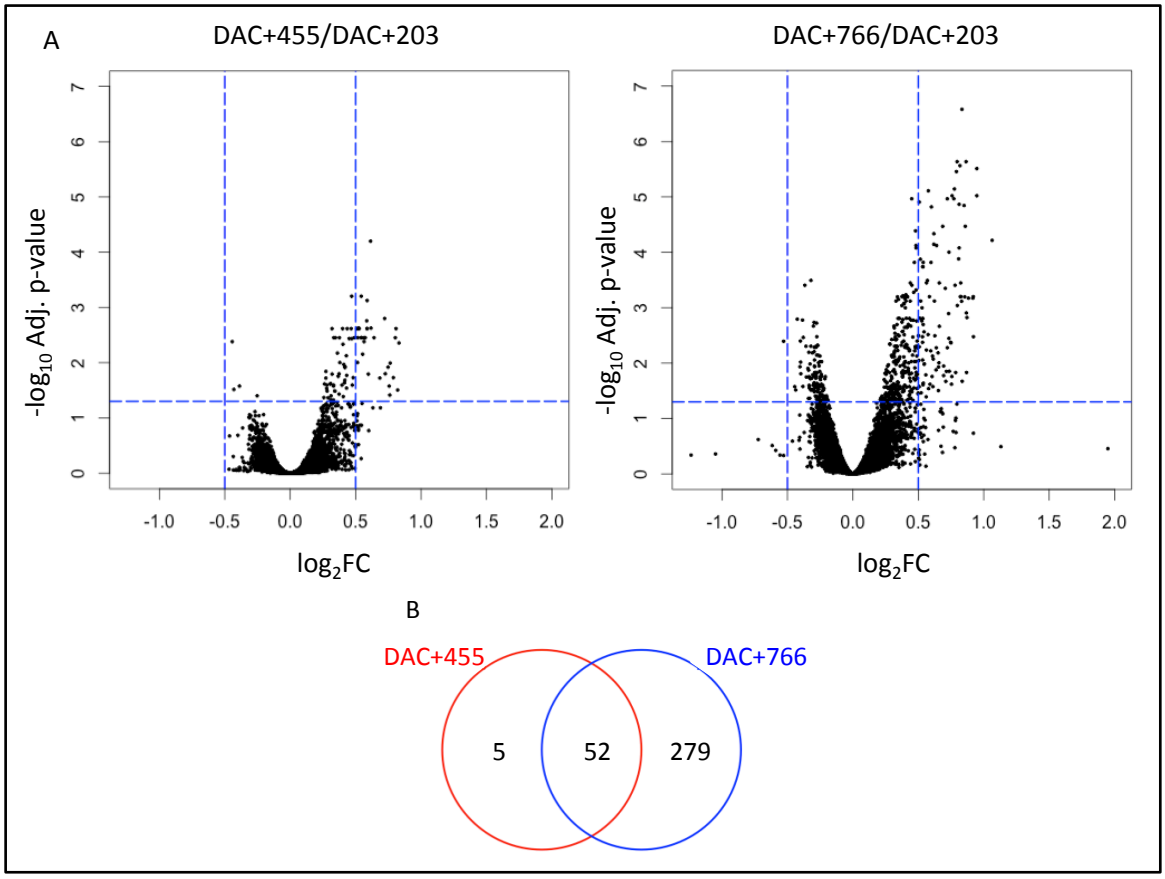

Figure 4-2. A. Volcano plots for gene expression changes for MCF-7 cells exposed to 62.5 nM DAC for 72 hours, followed by 9.375 uM KDM5 inhibitor for 72 hours relative to DAC+203. B. Venn diagram of overlap of differentially expressed genes following exposure to either active DAC+KDM5 inhibitor for 72hrs relative to DAC+203.

4.5.3 Figure 4-3. Active KDM5 inhibitor treatment results in significant differential gene expression patterns

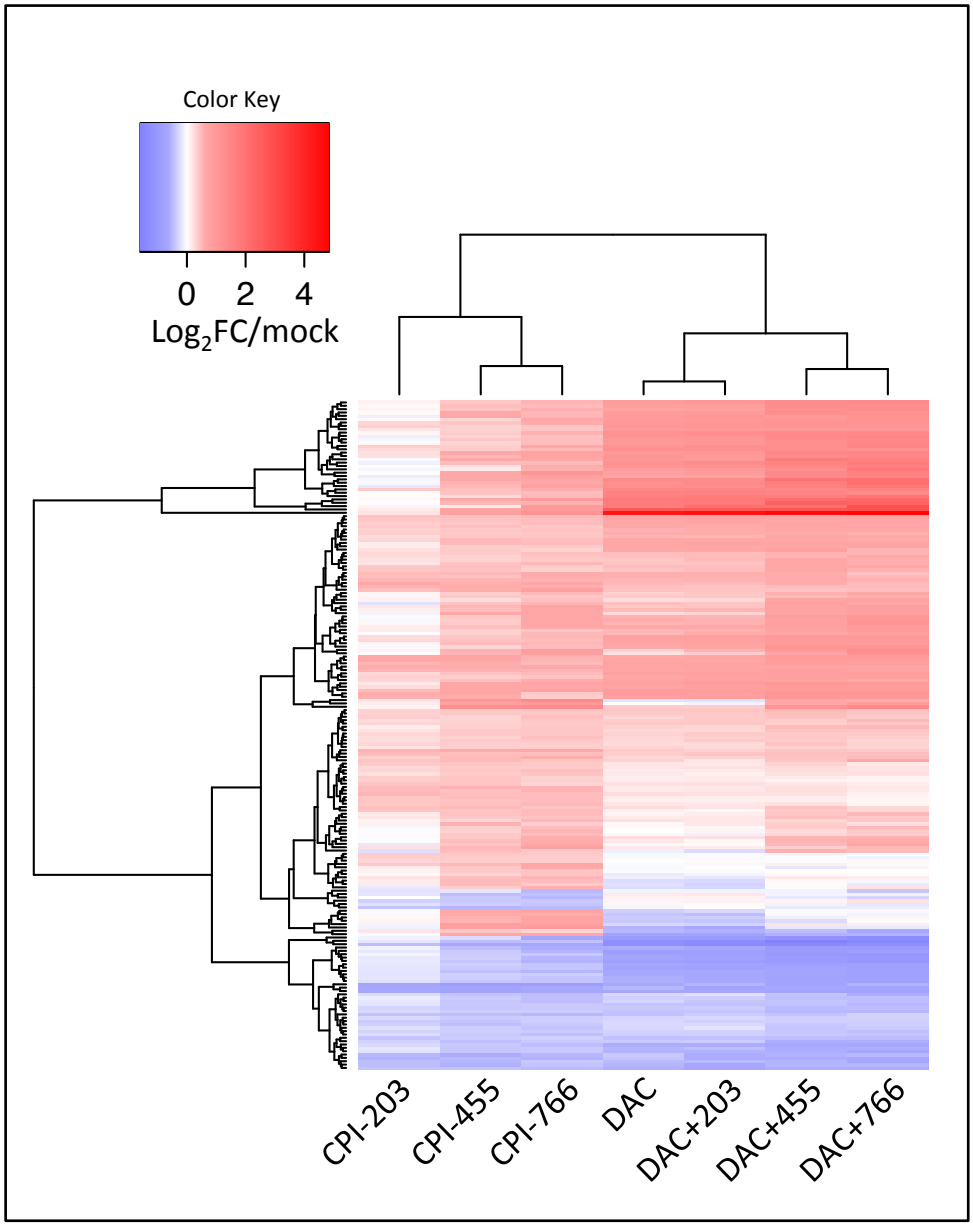

Figure 4-3. Clustering of various treatment groups exposed to indicated compounds based on the top 200 differentially expressed genes following treatment with CPI-455 or CPI-766. Intensity values shown represent log_2 fold change relative to treatment mock.

4.5.4 Figure 4-4. Combination treatment with DAC and KDM5 inhibitors results in significant differential expression patterns

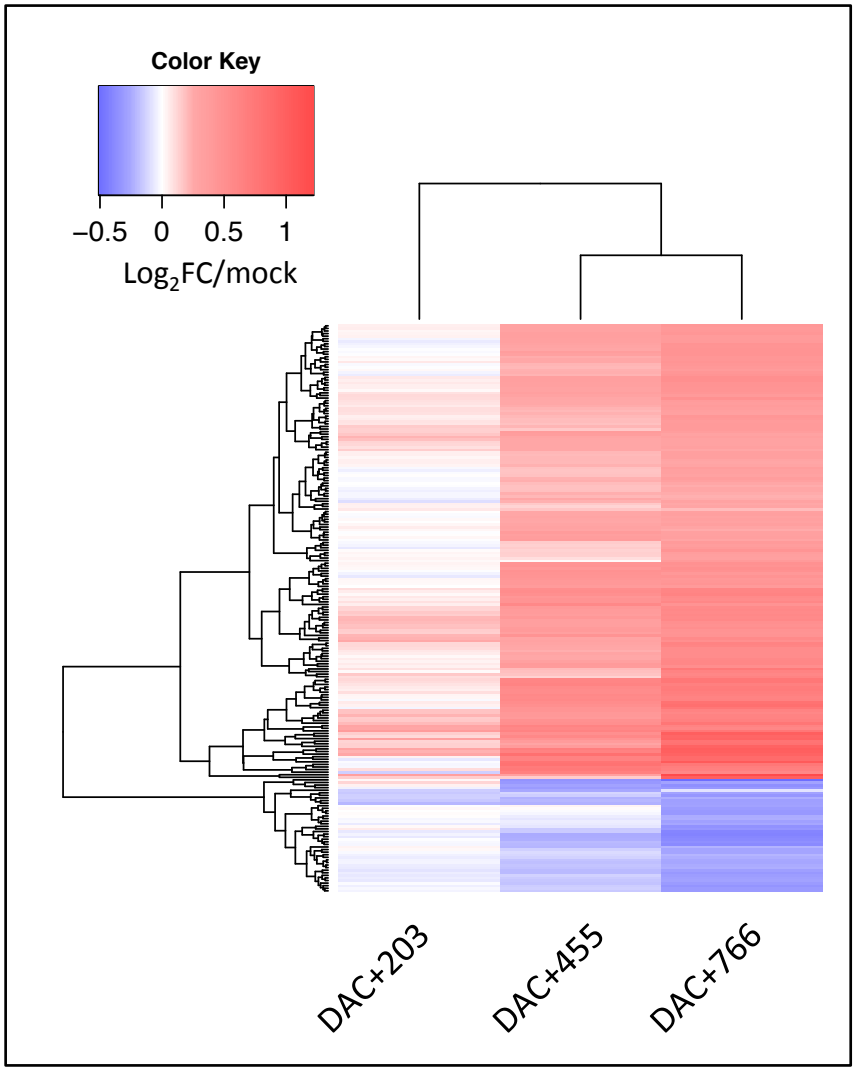

Figure 4-4. Clustering of combination treatment samples exposed to indicated compounds based all significantly differentially expressed genes (adj $p \leq 0.05$) following treatment with DAC+455 or DAC+766. Intensity values shown represent $\log_2$ fold change relative to treatment mock.

4.5.5 Figure 4-5. Genes significantly upregulated by KDM5 inhibitors are highly expressed in mock.

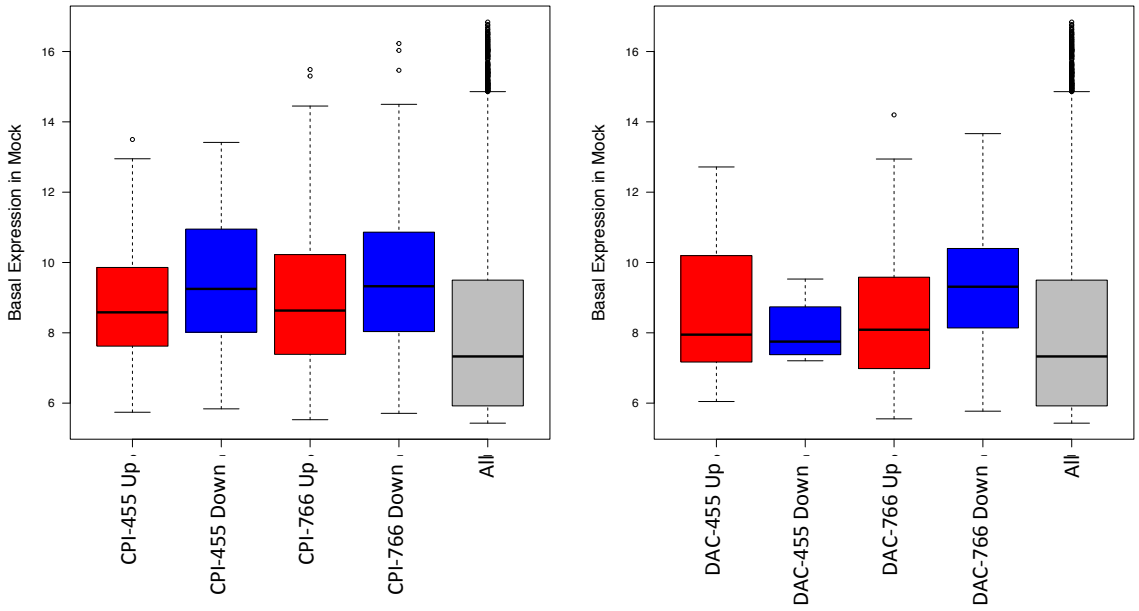

Figure 4-5. Basal expression rates in mock treated MCF-7 for genes differentially expressed following the indicated treatments compared to all genes probed on the microarray. Left panel: genes differentially expressed by KDM5 inhibitors alone relative to CPI-203. Right panel: genes differentially expressed by combination treatment relative to DAC+203.

4.5.6 Figure 4-6. Significantly enriched signaling pathways following KDM5 inhibitor treatment.

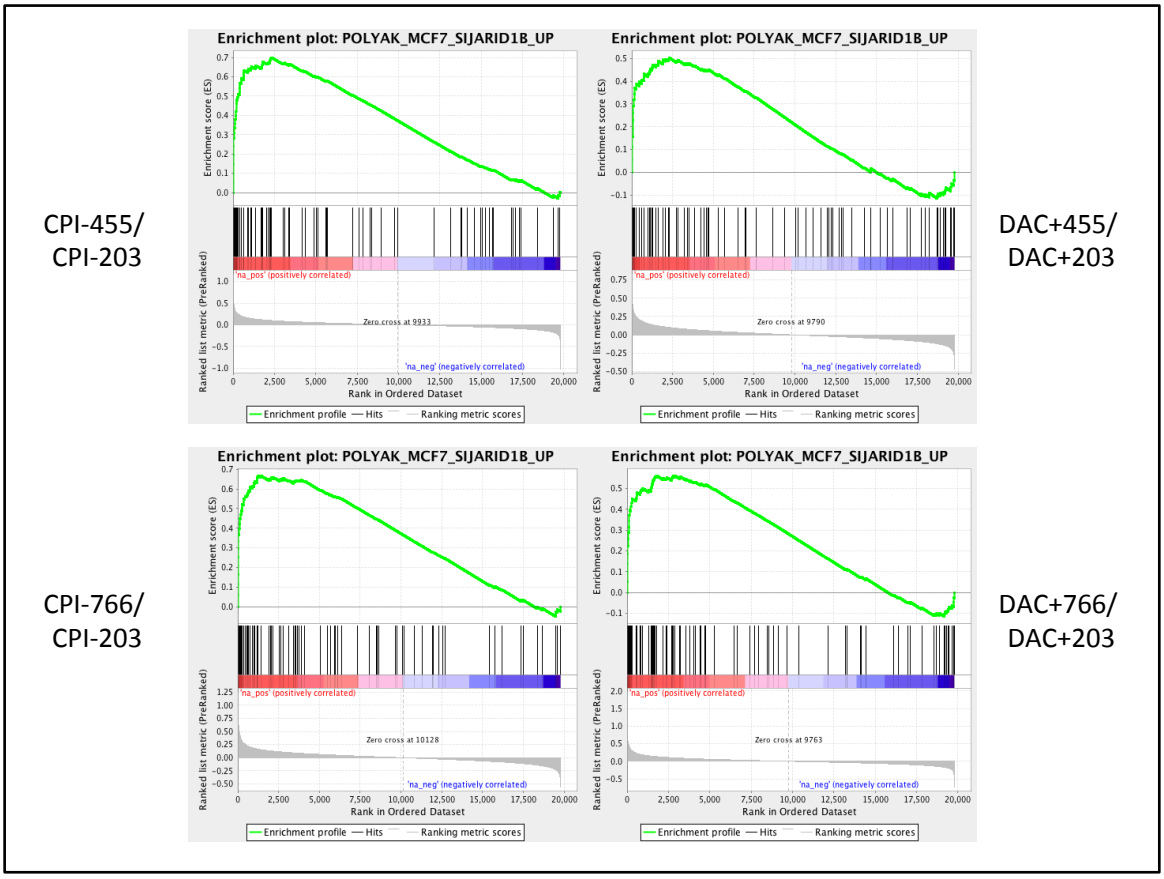

Figure 4-6a. Genes differentially expressed after KDM5 inhibitor treatment significantly enriched for targets upregulated after KDM5b siRNA. KDM5B siRNA up gene set obtained from Yamamoto et al. 2014

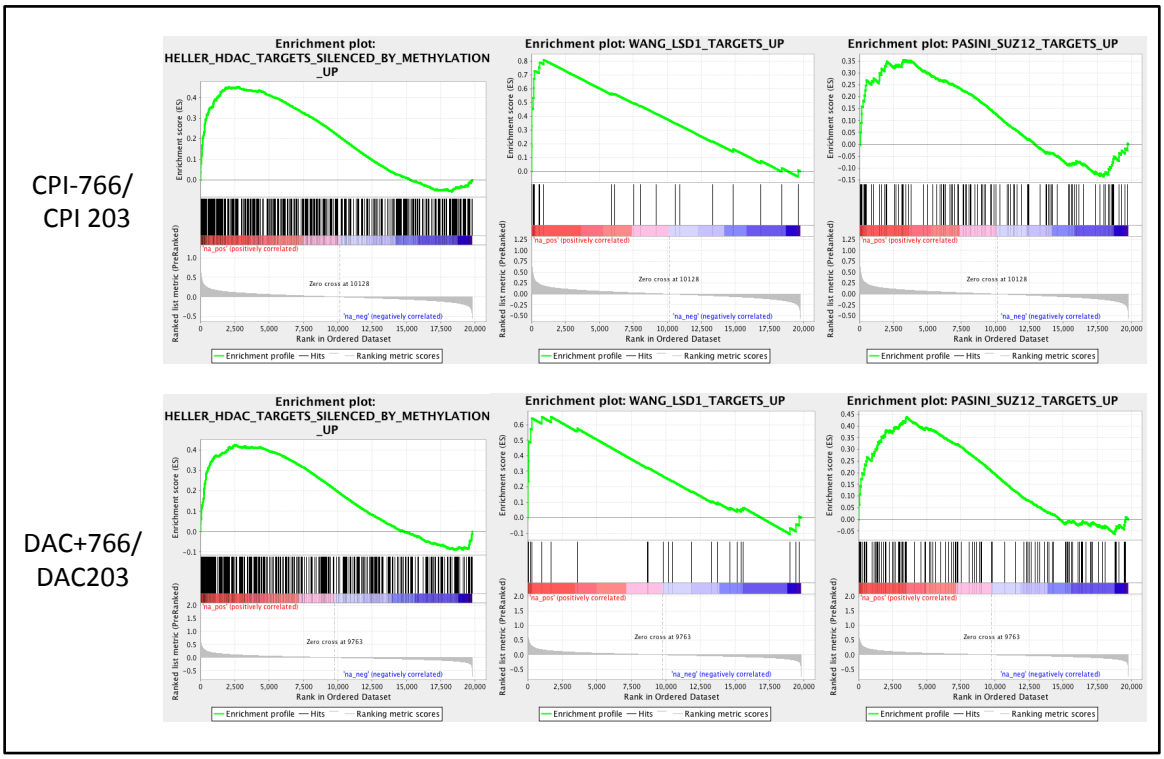

Figure 4-6b. Genes differentially expressed after KDM5 inhibitor treatment significantly enriched for targets upregulated after either combination treatment with DAC and the HDAC inhibitor trichostatin A or knockdowns of LSD1 or SUZ12.

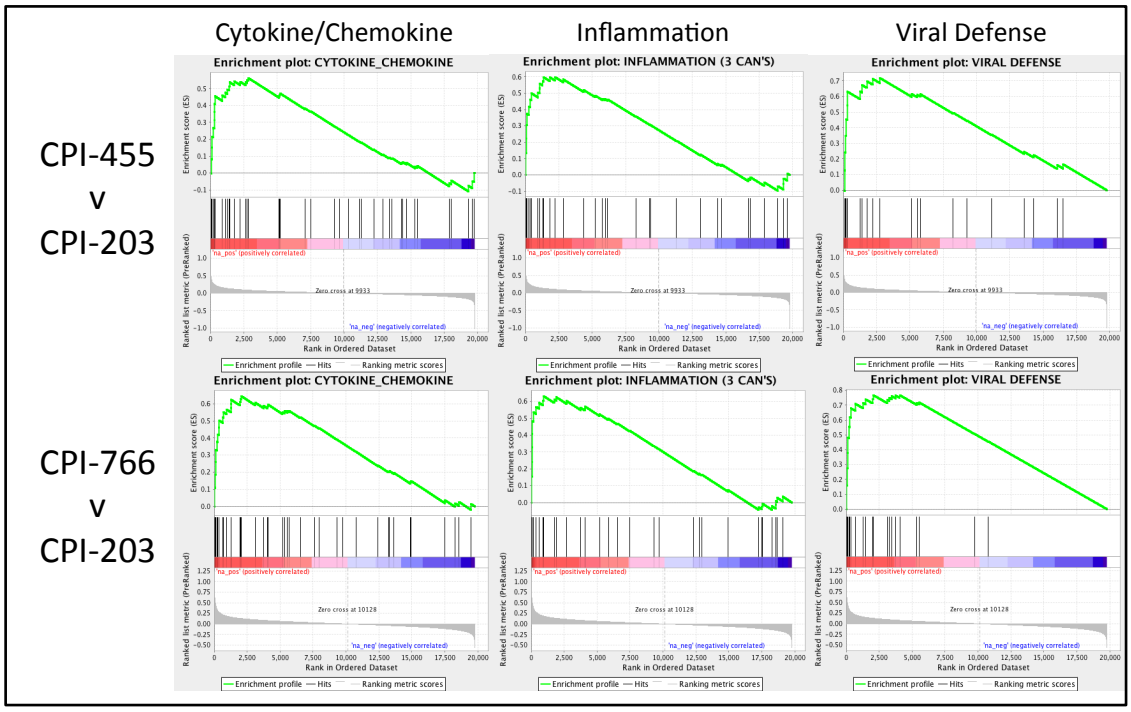

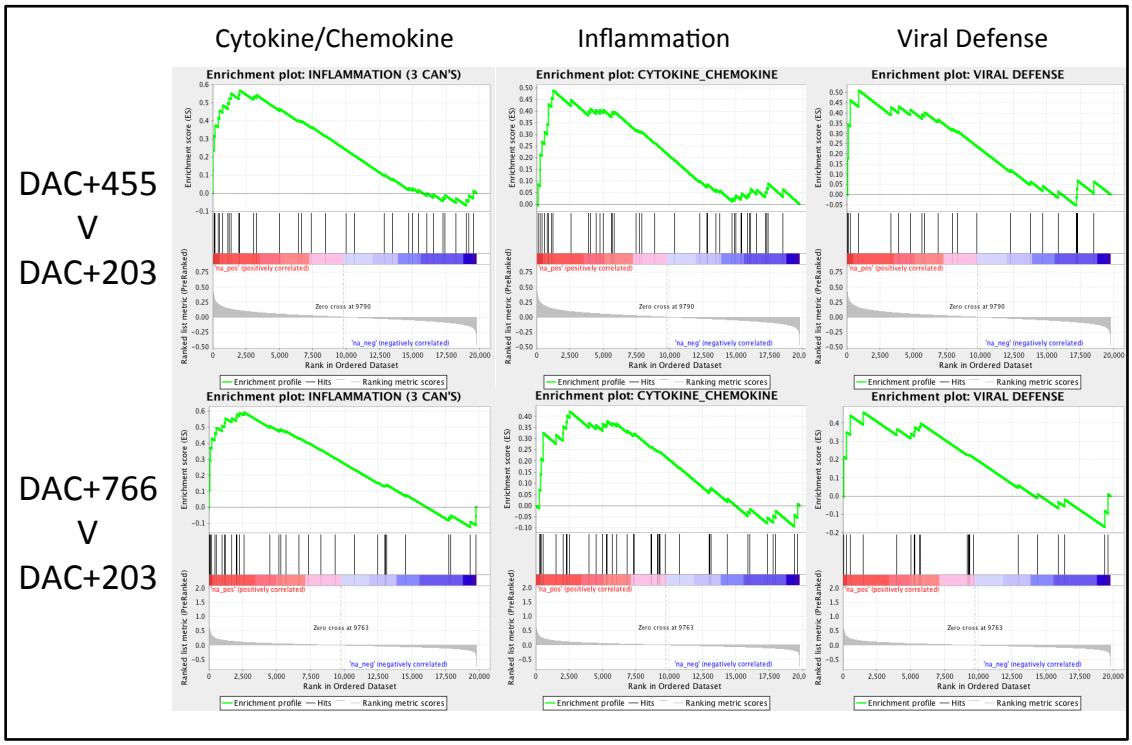

Figure 4-6c. Figure 4-6c. Genes differentially expressed after KDM5 inhibitor treatment significantly enriched for AIM pathways. Gene sets obtained from Li et al. 2014.

4.5.7 Figure 4-7. Global DNA methylation changes after KDM5 inhibitor treatment

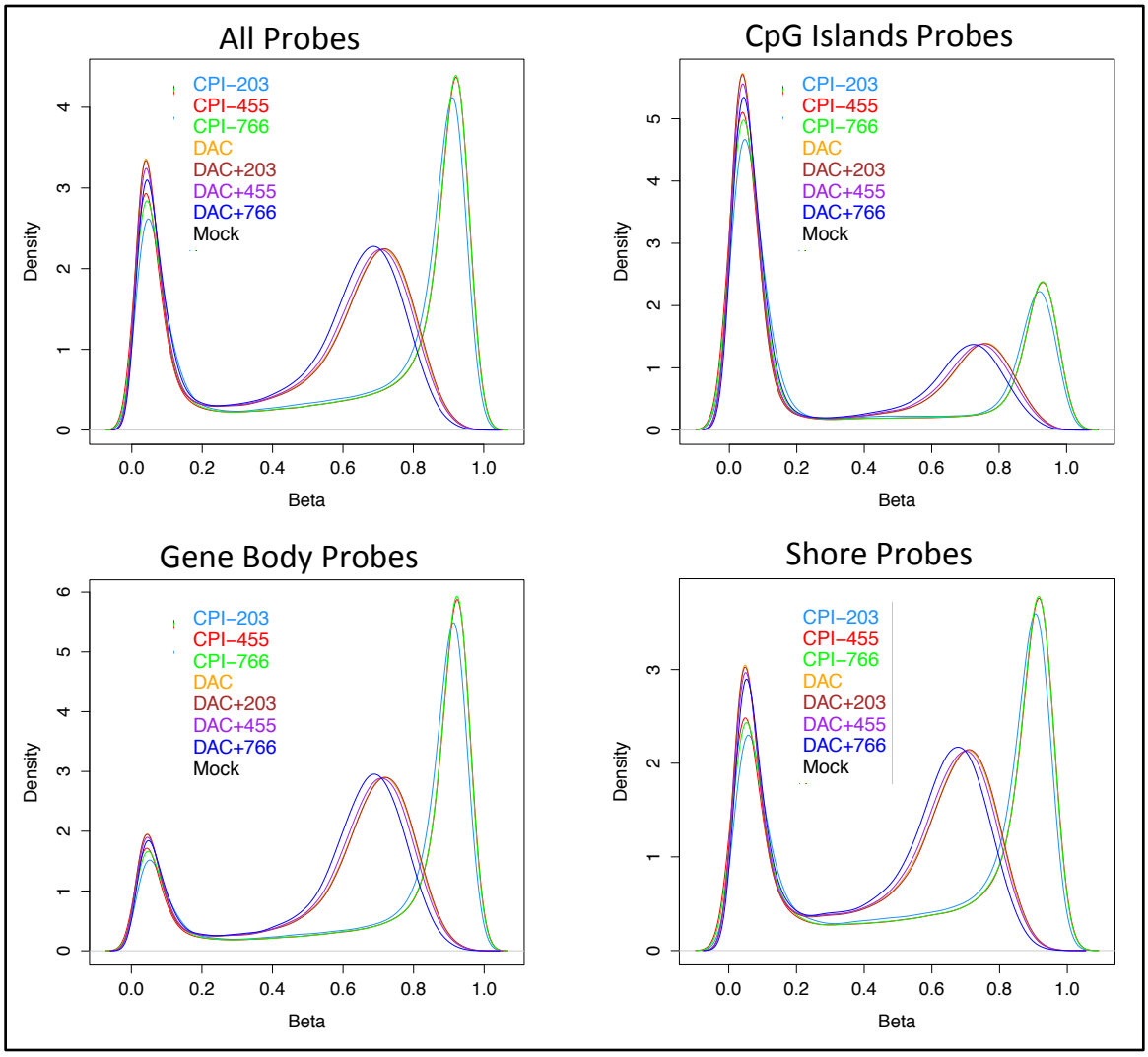

Figure 4-7. Beta-value density plots for MCF-7 cells treated with the indicated compounds. Density plots are shown for all, CpG island, gene body, and CpG shore probes.

4.5.8 Figure 4-8. KDM5 inhibitors significantly upregulate loci with promoter methylation

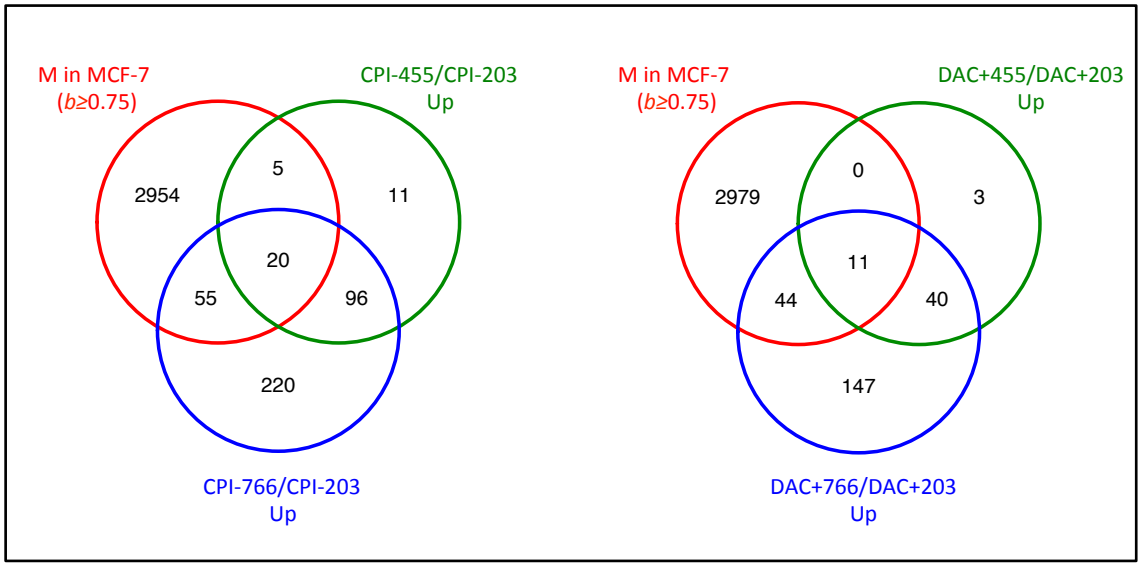

Figure 4-8. "M in MCF-7" indicates all genes with at least 1 CpG island probe with *b*>0.75 and within a window of -500 to +1500 bp from TSS. Left panel: overlap of methylated loci and genes upregulated by KDM5 inhibitors alone relative to CPI-203. Right Panel: overlap of methylated loci and genes upregulated by combination treatment relative to DAC+203.

4.5.9 Figure 4-9. Methylated KDM5 inhibitor targets are weakly repressed

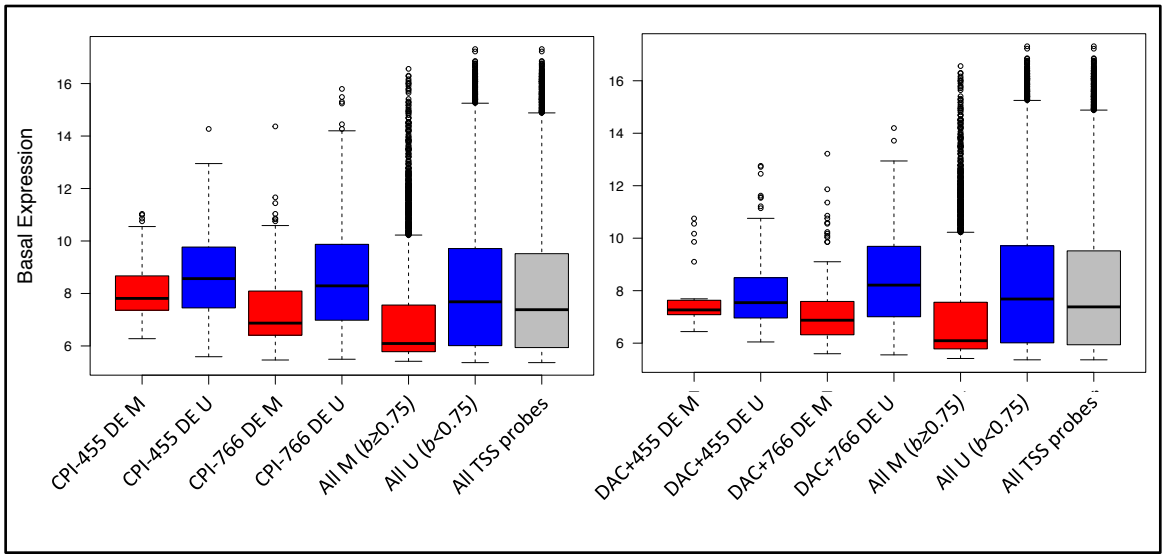

Figure 4-9. Shown are the basal expression rates in MCF-7 treatment mock samples for all differentially expressed genes based on methylation status. A gene was considered methylated, "M", if one CpG island probe with $b \geq 0.75$ was found within a window of -500 to +1500 bp from its TSS. Left panel: genes differentially expressed by KDM5 inhibitors alone relative to CPI-203. Right panel: genes differentially expressed by combination treatment relative to DAC+203.

4.5.10 Figure 4-10. KDM5 inhibitors do not affect DNA methylation of differentially expressed genes

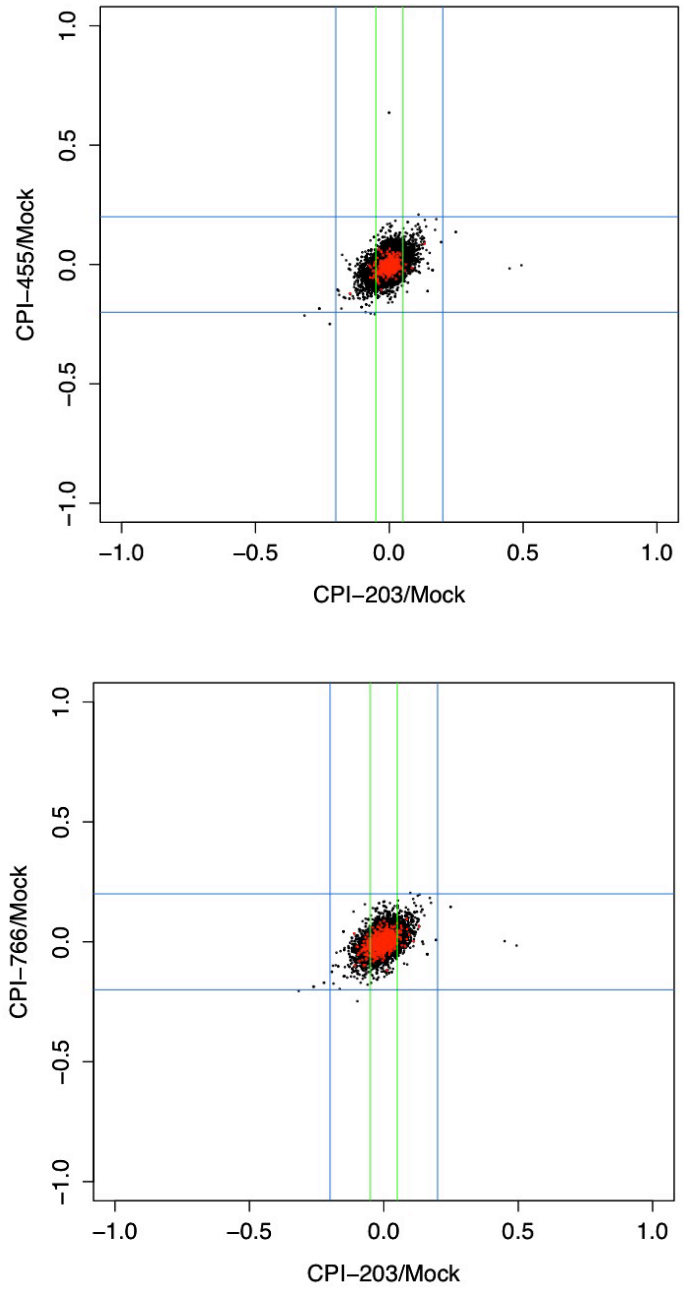

Figure 4-10. Delta beta values for active KDM5 inhibitors relative to treatment mock compared to CPI-203. Shown are all CpG island probes. All probes corresponding to significantly upregulated genes are highlighted in red.

4.5.11 Figure 4-11. Addition of KDM5 inhibitors to DAC treatment does not result in further DNA demethylation of differentially expressed genes.

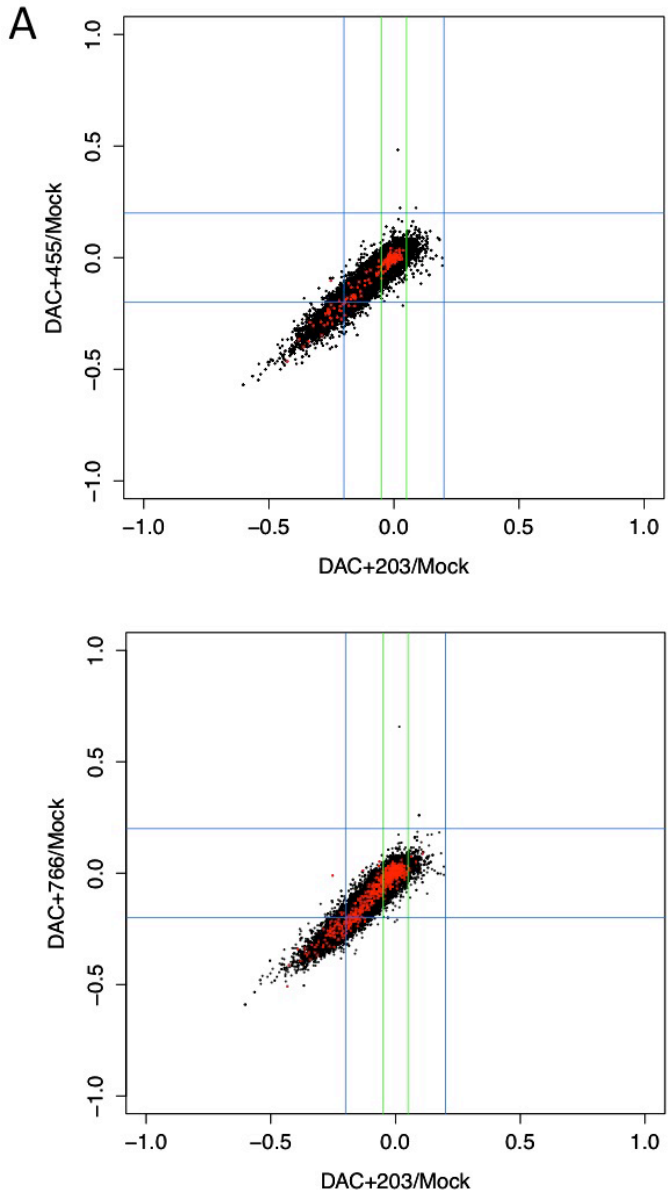

Figure 4-11a. Delta beta values for active combination relative to treatment mock compared to DAC+203. Shown are all CpG island probes. All probes corresponding to significantly upregulated genes are highlighted in red.

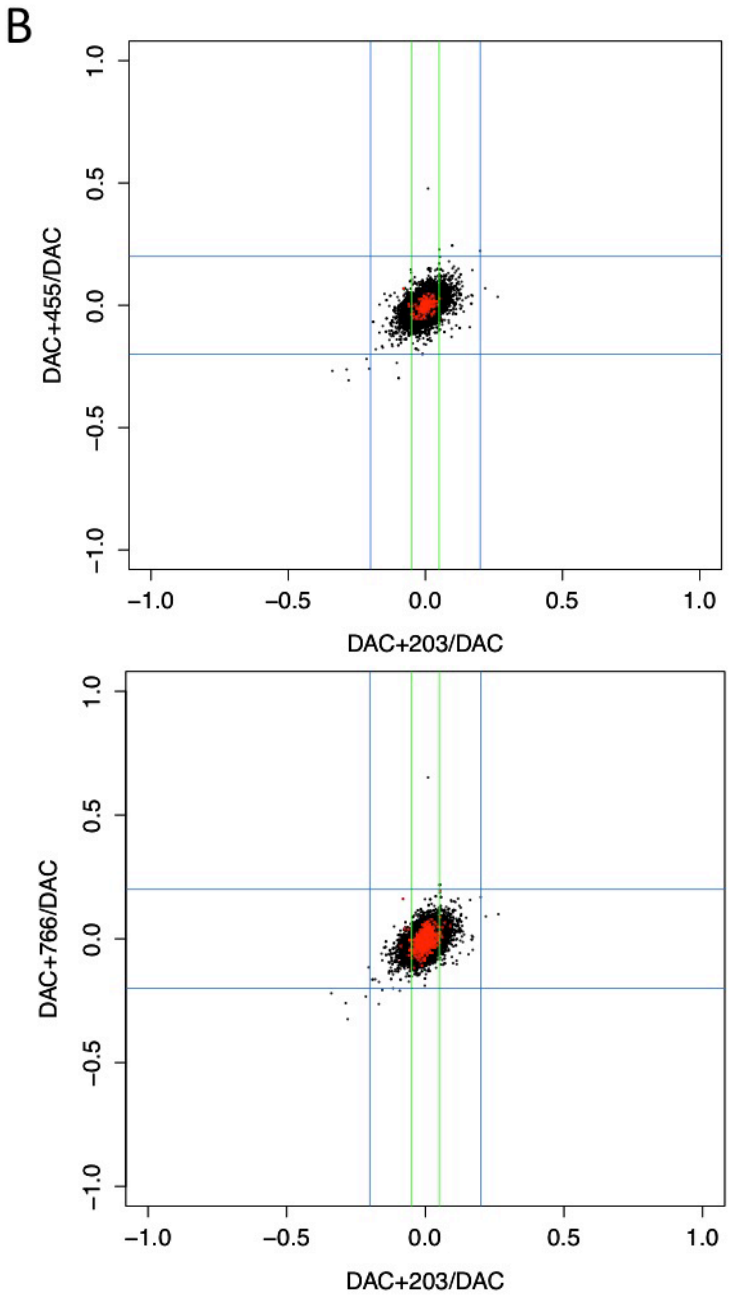

Figure 4-11b. Delta beta values for active combination relative to DAC alone compared to DAC+203 Shown are all CpG island probes. All probes corresponding to significantly upregulated genes are highlighted in red.

4.5.12 Figure 4-12. KDM5 inhibitors increase H3K4me3 levels at target promoters

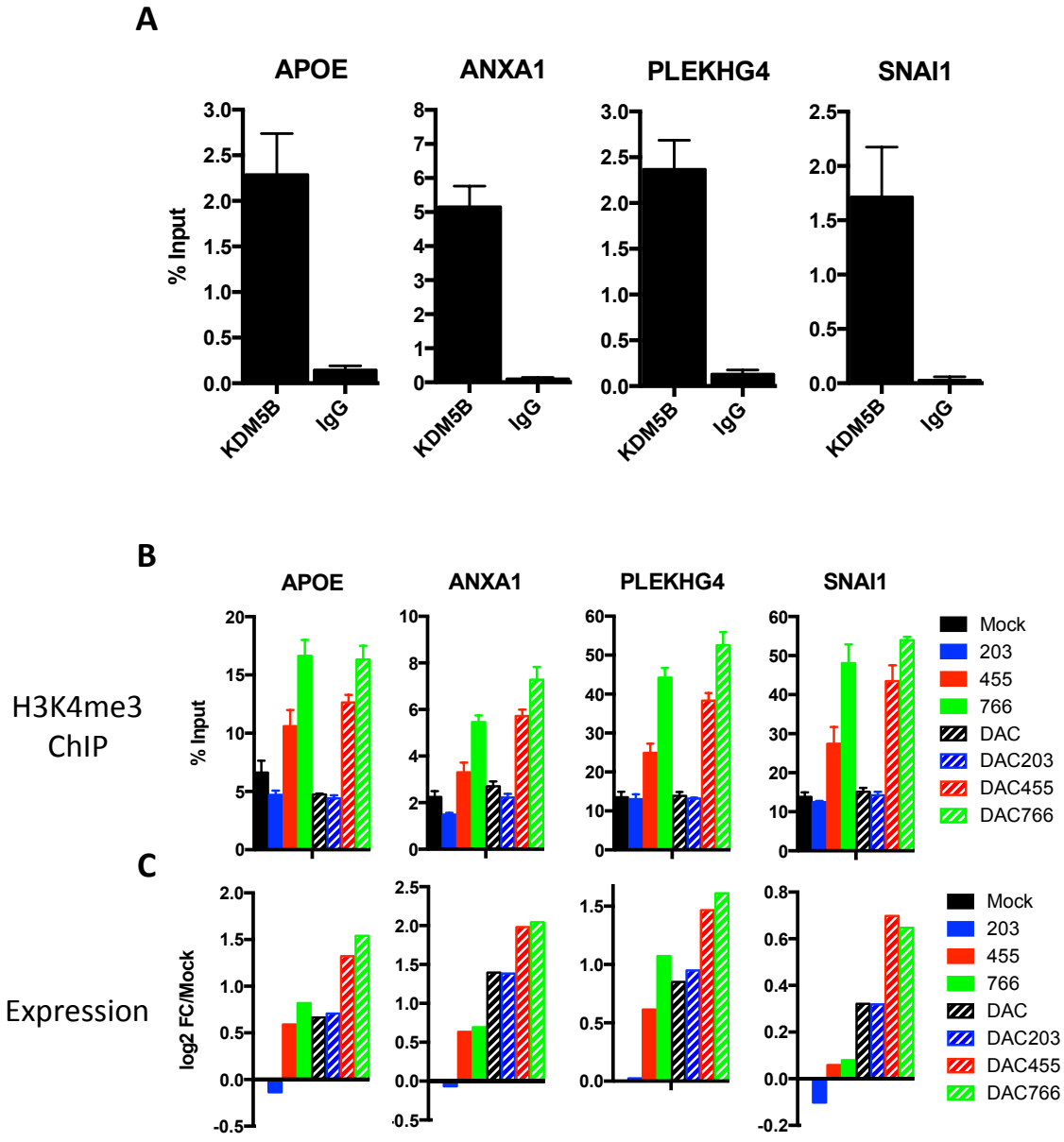

Figure 4-12. A. KDM5B enrichment at promoters of target genes calculated as percentage of input. B. H3K4me3 enrichment at target promoters calculated as percentage of input. C. Expression fold change compared to treatment mock. Data obtained from biological triplicates of expression microarray.

4.6 Tables: Chapter 4

4.6.1 Table 4-1. Significantly differentially expressed probes after treatment with KDM5 inhibitors alone or in combination with DAC.

	Diff. exp probes (adj. p≤0.05)	Unique genes
CPI-455/CPI-203	234	169
CPI-766/CPI-203	980	646
DAC+455/DAC+203	84	57
DAC+766/DAC+203	480	331

Table 3-1. Total number of significantly differentially expressed probes (adj. p≤0.05) following treatment with ether KDM5 inhibitors alone or in combination with DAC. Expression data for KDM5 inhibitors alone treatments was normalized to CPI-203, and data from combination treatments was normalized to DAC+203.

4.6.2 Table 4-2. Top differentially expressed genes following treatment with KDM5 inhibitors alone or in combination with DAC

CPI-455/CPI-203 Up	CPI-455/CPI-203 Down	CPI-766/CPI-203 Up	CPI-766/CPI-203 Down	DAC+455/DAC+203 Up	DAC+455/DAC+203 Down	DAC+766/DAC+203 Up	DAC+766/DAC+203 Down
MYO16	ZG16	PLEKHG4	MRS2	APOE	ZG16	APOE	HADHB
APOE	SPC25	APOE	CDC45	KLK8	MAP3K10	CYP24A1	AIFM1
MDK	BRCA1	MDK	BRCA1	EVPLL	NOVA1	CD36	ACAT1
CCDC83	FANCI	HCFC1R1	UBE2T	PLEKHG4	NAGPA	PLEKHG4	B3GNT1
LAMB2	CEP128	LAMB2	NFS1	LGALS1		EVPLL	RDX
PLEKHG4	GMNN	MYO16	TFF3	SPON2		LGALS1	WDHD1
HCFC1R1	MELK	PSCA	GOLGA2P5	CD36		PSG1	NFS1
PSCA	TTF2	KREMEN2	FAM156A	KRT13		LAMB2	LRRC75A
EVPLL	HOXB7	OBSCN	PCP4	MYO16		KLK8	SRR
TNFSF15	CENPW	CD36	HADH	CYP24A1		PSG9	ZG16
KREMEN2	MND1	CCDC83	TFF1	CRABP2		HEXIM2	DKK1
MAOA	CHMP4C	PSG1	MND1	STAT6		CCDC83	ATP5A1
IL17RE	CCNB1	EVPLL	WDHD1	LAMB2		TFPI	TSFM
ARHGEF19	UBE2T	FLRT3	MELK	CCDC83		KREMEN2	ABHD2
GEM	WDHD1	SLC6A14	CENPW	GPNMB		STAT6	OSBPL6
LGALS1	CENPN	TFPI	ABHD2	TNS4		CYP1B1	QTRT1
KCNJ13	LRP8	PALM3	CHMP4C	CTSV		HCFC1R1	CCDC34
PLLP	INCENP	LGALS1	CMC4	KREMEN2		WISP2	CMC4
FILIP1L	PHF19	CCDC88B	C11orf82	IL17RE		AKR1C3	KLHDC9
AQP3	FAM72A	STAT6	PIF1	FADS1		CCDC88B	TIPIN
OBSCN	TBC1D31	RHOBTB1	PBK	CYP4B1		MDK	RAD54L
STAT6	BLVRA	LMCD1	TBC1D31	NFE2		REM2	CAV2
S100A14	CDCA5	FSCN1	LIN54	RHOBTB3		OBSCN	MPV17
DEGS2	CHKB-AS1	UGT1A6	CENPH	ATP2B4		LMCD1	ZNF219
FLRT3	CDC45	PP14571	CEP128	SNAI1		COL9A3	LMO2
ZG16B	KCNS3	IGFBP2	INCENP	LDHD		P2RY6	NAGPA
TSPAN1	NINJ1	UGT1A8	ICAM3	ASPRV1		HMOX1	KRT37
ANXA1	KLHDC9	DBN1	FAM174A	CHST8		AKR1C1	RSAD1
PP14571	NTPCR	PSG9	QPCT	FSCN1		CRABP2	FAM47E
EPAS1	QPCT	TMEM80	CDCA5	ANXA1		TCHHL1	GALNT16
MYADM	FAM64A	CRABP2	CCNA2	HCFC1R1		FSCN1	PCP4
PALM3	BLM	HEXIM2	DBF4B	PKP1		FOLR1	FAM185A
RHOBTB3	RAD54L	YBX2	EFCAB11	AZGP1		SULT1A2	TFF3
PPP1R3C	NOVA1	TRIM47	BLM	SPTSSA		IRX4	PAGR1
UGT1A6	DLGAP5	ARHGEF19	C17orf58	PSG1		TNNC2	CYP2U1
DBN1	CCDC34	S100A14	CHAF1B	ARHGEF19		TNS4	C6orf211
LENG9	C11orf82	GEM	BUB1	ACACB		CFD	TRAP1
KRT13		EPAS1	DTL	ISYNA1		ZG16B	AVEN
CCDC88B		DLK2	PRR11	GPR87		TKT	PMP22
HMCN1		PLLP	BBX	PSG8		FTL	HOXC5
RGS9BP		VDR	NDC80	HEXIM2		IL17RE	NSMCE1
UGT1A8		PLEKHB1	TNNI2	PSORS1C1		ARHGAP4	MRPS28
WFDC2		ASCL2	ETFDH	BLNK		RHOBTB3	MCCC1
CXCR4		CYP1B1	C1QTNF9B-AS1	SLC30A3		ATP2B4	CCDC104
PSG1		WFDC2	DSCC1	ABCA12		TCEAL8	C10orf2
C11orf96		MAN1A1	BLVRA	GLA		NFE2	CLPB
LDHD		MAOA	CCDC84	MDK		CHST8	MPC1
CYP4B1		COL9A3	KNTC1	ASCL2		PALM3	NINJ1
TRIM47		ABCA12	GINS2	IL1RN		MB	MRS2
BLNK		ZG16B	SNRNP48	HMCN1		CTSV	LHFP

Table 4-2. Top up and down regulated genes with significant (adj. $p \leq 0.05$) differential expression after treatment with KDM5 inhibitors alone or in combination with DAC.

5. CHAPTER 5: CONCLUDING REMARKS

This work demonstrates that a novel set of inhibitors of KDM5 family of H3K4 demethylases synergistically enhance the effects of the well characterized, DNA hypomethylating agent, 5-aza-2'-deoxycytidine (DAC) in breast cancer cells. Here, we show that these new compounds lead to global and local increases in the transcriptionally activating histone mark, H3K4me3, without affecting cellular viability. But, when combined with DAC, these two classes of epigenetic inhibitors synergize to inhibit cell proliferation via an increased induction of apoptosis. To our knowledge, this is the first study demonstrating phenotypic synergy between the KDM5 family of histone demethylases and the DNA methylation machinery. Furthermore, as demonstrated in previous studies which combined other inhibitors of other epigenetic mechanisms, such as AZA plus HDAC inhibitors, or more recently AZA plus EZH2 inhibitors, our findings here indicate that the targeted inhibition of two distinct epigenetic mechanisms is a far more effective treatment paradigm than targeting either alone.

We next characterized the molecular effects induced by exposure to these compounds. We found that, not only did the KDM5 inhibitors result in the differential expression of hundreds of distinct loci, but that these compounds could also enhance the effects of DAC on transcriptional regulation, as the combination drug treatment lead to significant gene upregulation relative to DAC alone or DAC plus the inactive compound, CPI-203. Among these altered gene expression patterns was a significant upregulation of genes in AZA inducible immunomodulatory, or AIM, pathways. Genes in these pathways are normally lowly expressed in cancer to facilitate evasion of the immune

system, but are re-expressed upon AZA treatment, potentially making the cancer vulnerable to immune attack. Furthermore, re-expression of these genes could potentially sensitize cancer cells to immune checkpoint therapies, such as anti-PD1/PDL1 or anti-CTLA4, and this area is currently under investigation. Our observations indicate that treatment with the KDM5 inhibitors could further enhance the potential immune sensitization in the cancer cell following DAC treatment, thereby facilitating an increased vulnerability to immune checkpoint therapy. Future studies should address this question, as these findings could yield considerable clinical benefits in the management of patients with cancer.

These alterations in gene expression patterns appear to be driven by local changes to histone modifications at KDM5B targets. We initially proposed two alternative mechanisms; first, that the addition of KDM5 inhibitors to DAC treatment would facilitate further DNA demethylation at target promoters. Second, that by inhibiting the catalytic activity of KDM5 enzymes, H3K4me3 levels would increase at target loci, thereby facilitating an increase in transcription. Although slightly more DNA demethylation was observed in cells treated with DAC and CPI-766, we reject the first hypothesis as no differential methylation was observed at significantly upregulated targets (See Figs. 4-10 & 4-11). But, when exposed to the KDM5 inhibitors, either alone or in combination, we observed a substantial increase in H3K4me3 levels at differentially expressed loci. Interestingly, although transcription at these targets was upregulated in DAC treated samples, no significant changes in levels of this activating histone mark were observed (See Fig. 4-12). Given that three of the four loci tested contained no promoter DNA methylation, this observation indicates that transcriptional upregulation of

these targets following DAC exposure is likely mediated through the loss of repressive chromatin marks. Thus, the additive upregulation of expression of these targets in the samples exposed to DAC and the KDM5 inhibitors is likely the result of both the activating effects of local increases in H3K4me3 levels mediated by the KDM5 inhibitors, as well as the loss of repressive chromatin marks mediated by DAC exposure.

The above findings suggest that combinatorial inhibition of the KDM5 family and DNA methylation machinery could be of substantial clinical benefit. Here, we have shown the synergistic inhibition of growth in luminal breast cancer cells; it will be exciting if this observation is replicated in other cancer types. Furthermore, given that high KDM5B activity has been associated with decreased survival in hormone resistant breast cancer patients, our findings here indicate that these novel inhibitors of the KDM5 enzymes may represent a promising new therapeutic modality in the treatment of these tumors. Finally, recent studies have demonstrated that KDM5B expression is essential for the maintenance of a slow-cycling, stem-like cancer cell subpopulation that drives continuous tumor growth (Roesch et al. 2010). Chemical inhibition of KDM5 activity could potentially abrogate this slow-cycling subpopulation, thereby exhausting, and eventually halting tumor growth. In light of our findings here, therapeutic applications aimed at these targets warrant further investigation.

6. References

Aagaard, L. *et al.* (1999). Functional mammalian homologues of the *Drosophila* PEV-modifier Su(var)3–9 encode centromere-associated proteins which complex with the heterochromatin component M31. EMBO J. *18*, 1923–1938.

Aryee, M.J. *et al.* (2013). DNA Methylation Alterations Exhibit Intraindividual Stability and Interindividual Heterogeneity in Prostate Cancer Metastases. Sci. Transl. Med. *5*, 169ra10.

Astsaturov, I. *et al.* (2010). Synthetic lethal screen of an EGFR-centered network to improve targeted therapies. Sci. Signal. *3*, ra67.

Baylin, S.B. & Herman, J.G. (2000). DNA hypermethylation in tumorigenesis: Epigenetics joins genetics. Trends Genet. *16***,** 168–174.

Baylin,S.B. (2005). DNA methylation and gene silencing in cancer. Nat. Clin. Pract. Oncol., *2*, S4–S11.

Benevolenskaya, E.V. *et al.* (2005). Binding of pRB to the PHD Protein RBP2 Promotes Cellular Differentiation. Mol. Cell. 18, 623-635.

Bernstein, B. E. *et al.* (2006). A bivalent chromatin structure marks key developmental genes in embryonic stem cells. Cell. *125*, 315–326.

Bird, A. (2002). DNA methylation patterns and epigenetic memory. Genes Dev. *16*, 6–21.

Cai, Y *et al*. (2014) The NuRD complex cooperates with DNMTs to maintain silencing of key colorectal tumor suppressor genes. Oncogene. *33*, 2157-68.

Cameron, E. E. *et al*. (1999). Synergy of demethylation and histone deacetylase inhibition in the re-expression of genes silenced in cancer. Nature Genet. *21*, 103–107.

Cashen, A.C. *et al.* (2010). Multicenter, phase II study of decitabine for the first-line treatment of older patients with acute myeloid leukemia. J. Clin. Oncol. *28,* 556-561.

Clements, E.G. *et al*. (2012). DNMT1 modulates gene expression without its catalytic activity partially through its interactions with histone-modifying enzymes. Nucleic Acids Res. *40*, 4334-4346.

Cloos, P.A. *et al.* (2008) Erasing the methyl mark: histone demethylases at the center of cellular differentiation and disease. Genes Dev. *22*, 1115–1140.

Couture, J.F. *et al*. (2007). Specificity and mechanism of JMJD2A, a trimethyllysine-specific histone demethylase. Nat. Struct. Mol. Biol. *14*, 689-695.

Czermin, B. *et al.* (2002). *Drosophila* Enhancer of Zeste/ESC complexes have a histone H3 methyltransferase activity that marks chromosomal polycomb sites. Cell. *111*, 185–196.

De Smet, C. *et al*. (1999). DNA methylation is the primary silencing mechanism for a set of germ line- and tumor-specific genes with a CpG- rich promoter. Mol. Cell. Biol. *11*, 7327–7335.

Eden, A. *et al*. (2003) Chromosomal instability and tumors promoted by DNA hypomethylation. Science, *300*, 455.

Fahrner, J.A. *et al*. (2002). Dependence of histone modifications and gene expression on DNA hypermethylation in cancer. Cancer Res. *62*, 7213–7218.

Figueroa, M. E. *et al.* (2010). Leukemic IDH1 and IDH2 mutations result in a hypermethylation phenotype, disrupt TET2 function, and impair hematopoietic differentiation. *Cancer Cell. 18*, 553–567.

Fischle, W. *et al.* (2003). Molecular basis for the discrimination of repressive methyl-

lysine marks in histone H3 by Polycomb and HP1 chromodomains. Genes Dev. *17*, 1870–1881.

Fu, S. *et al.* (2011). Phase 1b–2a study to reverse platinum resistance through use of a hypomethylating agent, azacitidine, in patients with platinum- resistant or platinum-refractory epithelial ovarian cancer. Cancer. *117*, 1661–1669.

Greger, V. *et al*. (1989) Epigenetic changes may contribute to the forma-tion and spontaneous regression of retinoblastoma. Hum. Genet. *83*, 155–158.

Guenther, M. G. & Young, R. A. Transcription. Repressive transcription. Science. *329*, 150–151.

Halkidou, K. *et al*. (2004). Upregulation and nuclear recruitment of HDAC1 in hormone refractory prostate cancer. Prostate, *59*, 177–189.

Hayami, S. *et al.* (2010). Overexpression of the JmjC histone demethylase KDM5B in human carcinogenesis: involvement in the proliferation of cancer cells through the E2F/RB pathway. Mol Cancer. *9*, 59.

Hayami, S. *et al.* (2011). Overexpression of LSD1 contributes to human carcinogenesis through chromatin regulation in various cancers. Int. J. Cancer. *128*, 574-586.

Heller, G. *et al.* (2008). Genome-wide transcriptional response to 5-aza-2'-deoxycytidine and trichostatin a in multiple myeloma cells. Cancer Res. *68, 44-54.*

Holliday, R. (1987). The inheritance of epigenetic defects. Science. *238*, 163-70.

Issa,J.P. (2005). Optimizing therapy with methylation inhibitors in myelodysplastic syndromes: dose, duration, and patient selection. Nat. Clin. Pract. Oncol. *2*, S24–29.

Jaenisch, R. *et al.* (1985). Treatment of mice with 5-azacytidine efficiently activates silent retroviral genomes in different tissues. Proc. Natl. Acad. Sci. *82***,** 1451– 1455.

Juergens, R.A. *et al.* (2011). Combination epigenetic therapy has efficacy in patients with refractory advanced non-small cell lung cancer. Cancer Discov. *1*, 598–607.

Jones P.A. & Taylor S. (1980). Cellular Differentiation, Cytidine Analogs, and DNA methylation. Cell, *20*, 85-93.

Jones, P. A. & Baylin, S. B. (2002). The fundamental role of epigenetic events in cancer. Nature Rev. Genet. *3,* 415–428.

Jones, P.L. *et al*. (1998) Methylated DNA and MeCP2 recruit histone deacetylase to repress transcription. Nat. Genet. *19*, 187–191.

Kahl, P. *et al.* (2006). Androgen receptor coactivators lysine-specific histone demethylase 1 and four and a half LIM domain protein 2 predict risk of prostate cancer recurrence. Cancer Res. *66*, 11341-11347.

Klose, R.J. *et al.* (2007). The retinoblastoma binding protein RBP2 is an H3K4 demethylase. Cell. *128*, 889-900.

Komashko, V & Farnham, P.J. (2010). 5-azacytidine treatment reorganizes genomic histone modification patterns. Epigenetics. *5*, 229-240.

Kouzarides, T. (2007) Chromatin modifications and their function. Cell, *128*, 693–705.

Lambrot, R. & Kimmins, S. (2011). Histone methylation is a critical regulator of the abnormal expression of POU5F1 and RASSF1A in testis cancer cell lines. Int. J. Androl. *34,* 110-123.

Li, H. *et al.* (2014). Immune regulation by low doses of the DNA methyltransferase inhibitor 5-azacytidine in common human epithelial cancers. Oncotarget. *5,* 587-598.

Lin, W. *et al*. (2011). Loss of the retinoblastoma binding protein 2 (RBP2) histone demethylase suppresses tumorigenesis in mice lacking Rb1 or Men1. Proc. Natl. Acad.

Sci. *108*, 13379-13386.

McCabe, M.T. *et al*. (2012). EZH2 inhibition as a therapeu-tic strategy for lymphoma with EZH2-activating mutations. Nature. *492*, 108–112.

McGarvey, K.M. *et al.* (2008). Defining a chromatin pattern that characterizes DNA-hypermethylated genes in colon cancer cells. Cancer Res. *68, 5753-5759.*

Mikkelsen, T. S. *et al.* (2007). Genome-wide maps of chromatin state in pluripotent and lineage-committed cells. Nature. *448*, 553–560.

Nguyen, C.T. *et al*. (2002). Histone H3-lysine 9 methylation is associated with aberrant gene silencing in cancer cells and is rapidly reversed by 5-aza-2'-deoxycytidine. Cancer Res. *62*, 6456–6461.

Nelkin, B.D. *et al.* (1991). Abnormal methylation of the calcitonin gene marks progression of chronic myelogenous leukemia. Blood. *77*, 2431-2434.

O'Hagan, H. *et al.* (2011). Oxidative damage targets complexes containing DNA methyltransferases, SIRT1, and polycomb members to promoter CpG Islands. Cancer Cell. *20*, 606-19.

Ohm, J.E. *et al.* (2007). A stem cell-like chromatin pattern may predispose tumor suppressor genes to DNA hypermethylation and heritable silencing. Nat. Genet. *39,* 237-242.

Ooi, S.K. *et al.* (2007). DNMT3L connects unmethylated lysine 4 of histone H3 to *de novo* methylation of DNA. Nature. *448*, 714–717.

Pasini, D. *et al.* (2007). The polycomb group protein Suz12 is required for embryonic stem cell differentiation. Mol. Cell Biol. *27, 3769-3779.*

Peart, M. J. *et al*. (2005). Identification and functional significance of genes regulated by

structurally different histone deacetylase inhibitors. *Proc. Natl. Acad. Sci. 102*, 3697–3702.

Piekarz, R. L. *et al.* (2009). Phase II multi-institutional rial of the histone deacetylase inhibitor romidepsin as monotherapy for patients with cutaneous T-cell lymphoma. J. Clin. Oncol. *27*, 5410–5417.

Prendergast, G.C. *et al.* (1991) Methylation-sensitive sequence-specific DNA binding by the c-Myc basic region. Science. *251*, 186–189.

Ramalingam, S.S. *et al.* (2010). Carboplatin and paclitaxel in combination with either vorinostat or placebo for first-line therapy of advanced non-small-cell lung cancer. J. Clin. Oncol. *28*, 56–62.

Robert, C. & Rassool, F. V. (2012). HDAC inhibitors: roles of DNA damage and repair. Adv. Cancer Res. *116*, 87–129.

Rocchi, P. *et al*. (2005). p21Waf1/Cip1 is a common target induced by short-chain fatty acid HDAC inhibitors (valproic acid, tributyrin and sodium butyrate) in neuroblastoma cells. Oncol. Rep. *13*, 1139–1144.

Roesch, A. *et al*. (2010). A temporarily distinct subpopulation of slow-cycling melanoma cells is required for continuous tumor growth. Cell. *141*, 583-94.

Ruthenburg, A.J. *et al.* (2007). Methylation of lysine 4 on histone H3: intricacy of writing and reading a single epigenetic mark. Mol. Cell. *25,*15–30.

Scheubel, K.E. *et al.* (2007). Comparing the DNA hypermethylome with gene mutations in human colorectal cancer. PLoS Genet. *3,* 1709-1723.

Schlesinger, Y. *et al*. (2007) Polycomb-mediated methylation on Lys27 of histone H3 pre-marks genes for de novo methylation in cancer. Nat. Genet. *39*, 232–236.

Scibetta, A.G. *et al.* (2008). Functional analysis of the transcription repressor PLU-1/JARID1B. Mol. Cell Biol. *27,* 7220-7235.

Sengoku, T. & Yokoyama, S. (2011). Structural basis for histone H3 Lys 27 demethylation by UTX/KDM6A. Genes Dev. *25*, 2266-2277.

Shi, Y. *et al.* (2004). Histone demethylation mediated by the nuclear amine oxidase homolog LSD1. Cell. *119*, 941-953.

Solomon, J.M. *et al.* (2006). Inhibition of SIRT1 catalytic activity increases p53 acetylation but does not alter cell survival following DNA damage. Mol. Cell Biol. *26*, 28–38.

Song, J. *et al*. (2005). Increased expression of histone deacetylase 2 is found in human gastric cancer. APMIS. *113*, 264–268.

Suzuki, M.M. et al. (2008) DNA methylation landscapes: provocative insights from epigenomics. Nat. Rev. Genet. *9*, 465–476.

Tachibana, M. *et al.* (2005). Histone methyltransferases G9a and GLP form heteromeric complexes and are both crucial for methylation of euchromatin at H3-K9. Genes Dev. *19*, 815–826.

Tachibana, M. et al. (2008) G9a/GLP complexes independently mediate H3K9 and DNA methylation to silence transcription. EMBO J. *27*, 2681–2690.

Tsai, H.C. *et al.* (2011). Transient low doses of DNA-demethylating agents exert durable antitumor effects on hematological and epithelial tumor cells. Cancer Cell. *21*, 430-446.

Timmers, H. T. & Tora, L. (2005). SAGA unveiled. Trends Biochem. Sci. *30*, 7–10.

Valk-Lingbeek, M.E. *et al*. (2004). Stem cells and cancer; the polycomb connection. Cell. *118*, 409–418.

Wang, J. *et al.* (2007). Opposing LSD1 complexes function in developmental gene activation and repression programmes. Nature. *446, 882-887.*

Williams, K. *et al.* (2011). TET1 and hydroxymethylcytosine in transcription and DNA methylation fidelity. Nature. *473*, 343–348.

Wilson, A.S. *et al*. (2007) DNA hypomethylation and human diseases. Biochim. Biophys. Acta, *1775*, 138–162.

Wrangle, J. *et al*. (2013) Alterations of immune response of Non-Small Cell Lung Cancer with Azacytidine. Oncotarget. *4*, 2067-79.

Yamamoto, S. *et al.* (2014). JARID1B is a luminal lineage-driving oncogene in breast cancer. Cancer Cell. *25,* 762-777.

Yamane, K. *et al*. (2007). PLU-1 Is an H3K4 Demethylase Involved in Transcriptional Repression and Breast Cancer Cell Proliferation. Mol. cell. *25*, 801-812.

Yardley, D.A. *et al.* (2011). Results of ENCORE 301, a randomized, phase II, double-blind, placebo-controlled study of exemestane with or without entinostat in postmenopausal women with locally recurrent or metastatic estrogen receptor-positive (ER+) breast cancer progressing on a nonsteroidal aromatase inhibitor (AI). J. Clin. Oncol. *29*, 268.

Zeng, J. *et al.* (2010). The histone demethylase RBP2 Is overexpressed in gastric cancer and its inhibition triggers senescence of cancer cells. Gastroenterology. *138*, 981-992.

7. Appendix 1: PCR Primer Sequences

Primer Name	Sequence 5'-3'
KDM5B_RT1_F	ACTGCTTTCGTCAGGGAATC
KDM5B_RT1_R	GAAAATGATGTTGTGCCAGGAG
GAPDH_RT_F	GAAGGTCGGAGTCAACGGATTT
GAPDH_RT_R	ATGGGTGGAATCATATTGGAAC
APOE_ChIP_F	GGAGCCCTATAATTGGACAAG
APOE_ChIP_R	GGGTCCCAGCTCTTTCTA
ANXA1_ChIP_F	GTATGTCCCTAAAGTCACAGAATA
ANXA1_ChIP_R	TAATACCAGTGATTGGCACAC
PLEKHG4_ChIP_F	CCAGGTTCATGAAAGAGGTG
PLEKHG4_ChIP_R	GCGATTTGAGGTCCCTTTAG
SNAI1_ChIP_F	CCCAATCGGAAGCCTAACTA
SNAI1_ChIP_R	AACATCCTGTGACTCGATCC

Curriculum Vitae

Benjamin R. Leadem
509 South Bouldin St
Baltimore, Maryland 21224
(520) 245-8844
email: bleadem1@jhmi.edu

Education

- **Doctor of Philosophy:** Human Genetics and Molecular Biology. The Johns Hopkins School of Medicine. Baltimore, Maryland
    - May, 2015 (expected)
    - Thesis Title: " Novel histone demethylase inhibitors synergistically enhance the effects of a DNA hypomethylating agent in breast cancer cells"

- **Bachelor of Science**: Dual Majors in Biology and Psychology, Minor in Chemistry, May 2007; Northern Arizona University; Flagstaff, Arizona
GPA: 4.0/4.0

Research Experience

- **2008-present.** Graduate Student. The Johns Hopkins University School of Medicine; Baltimore, Maryland
    - Thesis Advisor: Stephen Baylin
    - The goal of my research was to characterize a novel set of chemical inhibitors of the KDM5 family of histone 3, lysine 4 (H3K4) demethylases, alone and in combination with the DNA demethyalting 5-aza-2'–deoxycytidine (DAC).
    - These compounds specifically increased H3K4 trimethylation levels, in a dose and time dependent fashion. Interestingly though, no effect on proliferation was observed at these doses of the KDM5 inhibitors.

- But, when combined with DAC, the KDM inhibitors synergistically inhibit growth and alter gene expression patterns in luminal breast cancer cells.
- Altered gene expression was at least partially driven by specific increases in H3k4 methylation at target loci.

- **2007-2008.** Research Technician. Northern Arizona University; Flagstaff, Arizona
  - Principal Investigator: Paul Keim
    - Conducted molecular genetics and evolution research on the bacterial pathogen *Burkholderia pseudomallei & Coxiella burnetii*

- **2004-2007.** Undergraduate Researcher. Northern Arizona University; Flagstaff, Arizona
  - Principal Investigator: Paul Keim
  - Conducted molecular genetics and evolution research on the bacterial pathogen *Burkholderia pseudomallei*

Teaching Experience

- **2012.** The Johns Hopkins University School of Medicine, Baltimore MD.
  - Teaching Assistantship: Advanced Topics in Human Genetics

- **2004-2006.** Supplemental Instructor: College of Engineering and Natural Sciences/ Learning Assistance Centers; Northern Arizona University, Flagstaff, Arizona
  - Supplemental Instructor: College of Engineering and Natural Sciences/ Learning Assistance Centers
  - Led group and individual tutoring sessions for introductory college-level Biology courses. Focus was not only on lecture material, but also developing effective learning/studying strategies.

Honors and Awards

- **Graduated Suma Cum Laude**: May, 2007
- **NAU College of Engineering and Natural Sciences Undergraduate Research Symposium (2007):** Awarded 1st place in College of Engineering and Natural Sciences Undergraduate Research Symposium, May, 2007.
- **Junior Scholastic Achievement Award**: Awarded by Northern Arizona University Biology Department; April 2006.
- **Dean's List:** 8 semesters (2003-2007), Northern Arizona University

Peer-reviewed publications

- Novel inhibitors of KDM5 family proteins synergize with DNMT inhibitors to regulate gene expression and inhibit proliferation of breast cancer cells. **Leadem BR,** Gehling VS, Harmange JC, Albrecht B, Trojer P, Classon M, Baylin SB. *In preparation*

- DNMT1 modulates gene expression without its catalytic activity partially through its interactions with histone-modifying enzymes. Clements EG, Mohammad HP, **Leadem BR,** Easwaran H, Cai Y, Van Neste L, Baylin SB. *Nucleic Acids Res*. 2012 May;40(10):4334-46. PMID: 22278882

- Loss of a single Hic1 allele accelerates polyp formation in Apc(Δ716) mice. Mohammad HP, Zhang W, Prevas HS, **Leadem BR**, Zhang M, Herman JG, Hooker CM, Watkins DN, Karim B, Huso DL, Baylin SB. *Oncogene*. 2011 Jun 9;30(23):2659-69. PMID: 21297660

- Within-host evolution of Burkholderia pseudomallei in four cases of acute melioidosis. Price EP, Hornstra HM, Limmathurotsakul D, Max TL, Sarovich DS, Vogler AJ, Dale JL, Ginther JL, **Leadem B**, Colman RE, Foster JT, Tuanyok A, Wagner DM, Peacock SJ, Pearson T, Keim P. *PLoS Pathog*. 2010 Jan 15;6(1):e1000725. PMID: 20090837

- Phylogeographic reconstruction of a bacterial species with high levels of lateral gene transfer. Pearson T, Giffard P, Beckstrom-Sternberg S, Auerbach R, Hornstra H, Tuanyok A, Price EP, Glass MB, **Leadem B**, Beckstrom-Sternberg JS, Allan GJ, Foster JT, Wagner DM, Okinaka RT, Sim SH, Pearson O, Wu Z, Chang J, Kaul R, Hoffmaster AR, Brettin TS, Robison RA, Mayo M, Gee JE, Tan P, Currie BJ, Keim P. *BMC Biol*. 2009 Nov 18;7:78. PMID: 19922616

- Identification of melioidosis outbreak by multilocus variable number tandem repeat analysis. Currie BJ, Haslem A, Pearson T, Hornstra H, **Leadem B**, Mayo M, Gal D, Ward L, Godoy D, Spratt BG, Keim P. *Emerg Infect Dis*. 2009 Feb;15(2):169-74. PMID: 19193259

- Genomic islands from five strains of Burkholderia pseudomallei. Tuanyok A, **Leadem BR**, Auerbach RK, Beckstrom-Sternberg SM, Beckstrom-Sternberg JS, Mayo M, Wuthiekanun V, Brettin TS, Nierman WC, Peacock SJ, Currie BJ, Wagner DM, Keim P. *BMC Genomics*. 2008 Nov 27;9:566. PMID: 19038032

- Fine-scale genetic diversity among Burkholderia pseudomallei soil isolates in northeast Thailand. U'ren JM, Hornstra H, Pearson T, Schupp JM, **Leadem B**, Georgia S, Sermswan RW, Keim P. *Appl Environ Microbiol.* 2007 Oct;73(20):6678-81. PMID: 17720819

- Tandem repeat regions within the Burkholderia pseudomallei genome and their application for high resolution genotyping. U'Ren JM, Schupp JM, Pearson T, Hornstra H, Friedman CL, Smith KL, Daugherty RR, Rhoton SD, **Leadem B**, Georgia S, Cardon M, Huynh LY, DeShazer D, Harvey SP, Robison R, Gal D, Mayo MJ, Wagner D, Currie BJ, Keim P. *BMC Microbiol*. 2007 Mar 30;7:23. PMID: 17397553

- VNTR analysis of selected outbreaks of Burkholderia pseudomallei in Australia. Pearson T, U'Ren JM, Schupp JM, Allan GJ, Foster PG, Mayo MJ, Gal D, Choy

JL, Daugherty RL, Kachur S, Friedman CL, **Leadem B**, Georgia S, Hornstra H, Vogler AJ, Wagner DM, Keim P, Currie BJ. *Infect Genet Evol*. 2007 Jul;7(4):416-23. PMID: 17258514

Presentations

- **Keystone Symposium on Molecular and Cellular Biology: DNA Methylation.** Invited short lecture: "Novel inhibitors of KDM5 family proteins synergize with DNMT inhibitors to regulate gene expression and inhibit proliferation of breast cancer cells". Keystone, Colorado. April 2015

- **Keystone Symposium on Molecular and Cellular Biology: DNA Methylation.** Poster presentation: "Novel inhibitors of KDM5 family proteins synergize with DNMT inhibitors to regulate gene expression and inhibit proliferation of breast cancer cells". Keystone, Colorado. April 2015

- **American Society of Microbiologists General Meeting 2007:** Poster presentation**: "**MLVA and MLST: a Multiple Marker Approach for Progressive Hierarchical Analysis of *Burkholderia pseudomallei*" Toronto, ON; May, 2007

- **American Society of Microbiologists Regional Meeting 2007:** Short lecture: **"**MLVA and MLST: a Multiple Marker Approach for Progressive Hierarchical Analysis of *Burkholderia pseudomallei*"; Flagstaff, AZ; April 2007

- **CENS Undergraduate Research Symposium 2007:** Poster presentation: "MLVA and MLST: a Multiple Marker Approach for Progressive Hierarchical Analysis of *Burkholderia pseudomallei*"; Northern Arizona University, Flagstaff Arizona; April, 2007

- **CENS Undergraduate Research Symposium 2006: :** Poster Presentation: "Multiple-Locus Variable-Number Tandem Repeat Analysis Reveals Genetic

Diversity Among Human and Soil Isolates of *Burkholderia pseudomallei* from Northeast Thailand"; Northern Arizona University, Flagstaff Arizona; May, 2006

- **CENS Undergraduate Research Symposium 2005:** Poster Presentation: **"**Analysis of Single Nucleotide Repeats in Burkholderia pseudomallei" Northern Arizona University, Flagstaff Arizona, May, 2005

Additional meetings attended

- **NCI Symposium on Chromosome Biology: Chromatin, ncRNA, Methylation & Disease.** Bethesda, Maryland. 2013

- **50th Annual Short Course on Medical and Experimental Mammalian Genetics**. The Jackson Laboratory. Bar Harbor, Maine. 2009

References

Stephen Baylin, M.D. sbaylin@jhmi.edu
Virginia and D.K. Ludwig Professor 410-955-8506
Deputy Director, The Sydney Kimmel Comprehensive Cancer Center at Johns Hopkins.
Professor of Oncology and Medicine
The Johns Hopkins University

James Herman, M.D. hermanj3@upmc.edu
Co-leader, UPCI Lung Cancer Program 412-623-7769
Professor of Medicine
The University of Pittsburgh